https://doi.org/10.5194/gmd-2021-88
Preprint. Discussion started: 25 May 2021


Geoscientific Model Development Discussions

# An emergency response model for evaluating the formation and dispersion of plumes originating from major fires (BUOYANT v4.20)

Jaakko Kukkonen[1], Juha Nikmo[1], Kari Riikonen[1], Ilmo Westerholm[1], Pekko Ilvessalo[1], Tuomo Bergman[1] and Klaus Haikarainen[1]

[1]Finnish Meteorological Institute, Erik Palménin aukio 1, P.O. Box 503, 00101, Helsinki, Finland

*Correspondence to*: Jaakko Kukkonen (jaakko.kukkonen@fmi.fi)

**Abstract.** A mathematical model called BUOYANT has previously been developed for the evaluation of the dispersion of positively buoyant plumes originating from major warehouse fires. The model addresses the variations of the cross-plume integrated properties of a rising plume in a vertically varying atmosphere and the atmospheric dispersion after the plume rise regime. We have described in this article an extension of the BUOYANT model to include a detailed treatment of the early evolution of the fire plumes, before the plume rise and atmospheric dispersion regimes. The model input and output consist of selected characteristics of forest or pool fires, and the properties of a source term for the plume rise module, respectively. The main model structure of this source term model is based on the differential equations for low-momentum releases of buoyant material, which govern the evolution of the plume radius, velocity and density differences. The model is also partially based on various experimental results on fire plumes. We have evaluated the refined BUOYANT model by comparing the model predictions against the experimental field-scale data of the Prescribed Fire Combustion and Atmospheric Dynamics Research Experiment, RxCADRE. The predicted concentrations of $CO_2$ agreed fairly well with the aircraft measurements conducted in the RxCADRE campaign. We have also compiled an operational version of the model. The operational model can be used for emergency contingency planning and for the training of emergency personnel, in case of major forest and pool fires.

## 1 Introduction

The dispersing fire plumes can represent a substantial hazard on the health of people and the state of the environment, in addition to the direct effects of major fires at the accident sites. Major fires include, e.g., fires in warehouses and industrial sites, and wildland fires. The latter category includes, e.g., heath, moorland and forest fires. Major wildland fires can result in substantially more extensive and intensive

https://doi.org/10.5194/gmd-2021-88
Preprint. Discussion started: 25 May 2021


fire plumes, compared with industrial and warehouse fires. The pollutants from wildland fires are commonly transported in the troposphere, but may in some cases reach the stratosphere (e.g., Freitas et al., 2007; Sofiev et al., 2012). The most important process in describing the plume dispersion from major fires can be considered to be the initial plume rise (e.g., Liousse et al., 1996; Trentmann et al., 2002; Kukkonen et al., 2014). Overviews of buoyant plume models have been presented, for example, by Devenish et al. (2010) and Jirka (2004).

The emissions from wildland fires can affect human health, the state of ecosystems, carbon stocks, and land surface reflectance. Solid fuels, such as vegetative biomass, are consumed in a two-stage process including pyrolysis and combustion (Ottmar, 2014). Pyrolysis is the chemical decomposition of a solid material by heating, and it results in gaseous and solid products (Ottmar, 2014; Rein, 2016). Pyrolysis is an endothermic process, and by definition, it does not involve combustion reactions. Although both stages occur nearly simultaneously, pyrolysis occurs first, followed by oxidation of the escaping hydrocarbon vapours (Ottmar, 2014; Rein, 2016).

Combustible liquids are during burning commonly first converted from liquid to vapour, without any chemical decomposition of fuel molecules (Drysdale, 2016). Exceptions to this general rule include high molecular weight liquids, which may be subject to chemical decomposition at temperatures associated with vapour formation (Drysdale, 2016). In the atmosphere, air is mixed and reacts with the flammable vapours that are evaporated from the liquid surface; this is called burning as a diffusion flame. Complete combustion is rarely achieved in atmospheric conditions; commonly products of incomplete combustion will therefore be formed, such as carbon monoxide and smoke (Khan et al., 2016). Hundreds of chemical compounds are emitted into the atmosphere during wildland fires (Ottmar, 2014).

In realistic simulations of air quality and climate, one needs to include wild-land fire emission models or inventories (e.g., Saarnio et al., 2010; Sofiev et al., 2009; Wiedinmyer et al., 2006). The available estimation methods on a global scale have been addressed by, e.g., Hoelzemann et al. (2004), Ito and Penner (2004) and van der Werf et al. (2003). These inventories include fires at varying horizontal resolutions, from 1 km to 1° (latitude and longitude), and typically use a monthly temporal resolution. Wild-land fire emission predictions have been made also for specific episodes, fires, and regions (e.g., Dennis et al., 2002; Lavoué et al., 2000; Soja et al., 2004; Anderson et al., 2004).

https://doi.org/10.5194/gmd-2021-88
Preprint. Discussion started: 25 May 2021


Both inventory-type and satellite-based estimates of wildland fires may use as input values the burned area, fuel loads, and combustion completeness to calculate emissions (Seiler and Crutzen, 1980). However, studies using satellite-measured fire radiative power (FRP) do not require these input datasets. Such methods directly integrate FRP to the total fire radiative energy (FRE), which is in turn related to total emissions (Sofiev et al., 2009, van der Werf et al., 2010). Some studies have collected data sets that include fuel characteristics and consumption, and environmental variables, regarding both wildfires and prescribed fires (Ottmar, 2014). These datasets have been used for fuel consumption models, such as Consume (Prichard et al., 2007), FOFEM (Reinhardt et al., 1997), and BORFIRE (de Groot et al., 2007 and 2009).

Semi-empirical and computational fluid dynamics (CFD) models have been used for the modelling of liquid pool fires (Rew and Hulbert, 1996; Brambilla and Manca, 2009). Semi-empirical models use heat transfer principles and dimensional analysis to evaluate, e.g., the fuel burning rate, the fraction of radiative power and the flame length. The CFD models for liquid pool fires solve the Navier-Stokes equations of fluid flow, together with treatments for the chemical and physical processes occurring in fires. There are numerous studies on hydrocarbon pool fires, including both experimental data (Mudan, 1984; Koseki, 1989; Luketa-Hanlin, 2006; Raj, 2007b; Fingas, 2014; Beyler, 2016) and theoretical analyses (Hottel, 1959; Hertzberg, 1973; Babrauskas, 1983; Hostikka et al., 2003; Fay, 2006; Raj, 2007a).

The modelling in this study is partly based on previous work by Ramsdale et al. (1997) and Kukkonen et al. (2000). The mathematical description of the modelling of plume rise and near-field dispersion was reported in Martin et al. (1997), and the larger-scale dispersion was addressed by Nikmo et al. (1997 and 1999). A mathematical model called BUOYANT has been developed, partly based on these previous studies; a previous version of this model has been described in detail by Kukkonen et al. (2014). The model is applicable for evaluating the initial plume rise and atmospheric dispersion of pollutants originated from strongly buoyant sources.

The input data for the BUOYANT model has included various meteorological parameters and information on the properties of the fire and its surroundings (Kukkonen et al., 2014). However, a reliable

https://doi.org/10.5194/gmd-2021-88
Preprint. Discussion started: 25 May 2021


evaluation of the required input data is a challenging task. Clearly, this has also up to date been the case for all other models for the dispersion of buoyant plumes from major fires. The application of such models has therefore been possible only for expert users.

The overarching aim of this study has been to develop a comprehensive model for evaluating the dispersion of plumes originating from major fires, including all the relevant dispersion regimes. An objective has been to develop an operational and user-friendly model for this purpose. The objective has been that such an operational model could be used also by well-trained meteorologists and by trained emergency rescue personnel. We have therefore developed a novel semi-empirical model for evaluating the initial conditions (i.e., source term) for models that treat the buoyant plume rise and the subsequent atmospheric dispersion of plumes from major fires. The input data required by the source term model is substantially simpler than the corresponding input required by the original model version.

The specific objectives of this study are the following. (i) The first objective is to present a new model for evaluating the initial properties of fire plumes in terms of fairly simple characterizations of major fires. We have also included the developed source term model to the BUOYANT model. (ii) The second objective is to compare the predictions of the latest version of the BUOYANT model against available field-scale experimental data. (iii) The third objective is to present the structure and functioning of the developed operational emergency response model. Both the original research model and its operational application could in the future be used worldwide, the latter after some slight modifications, for a better preparedness and rescue operations in case of major fires.

## 2 Model

For readability, we present first a brief overview of the whole modelling system. Second, we address the extension of the system to include source term evolution.

### 2.1 Overview of the modelling system

The BUOYANT model is applicable for evaluating the initial plume rise and atmospheric dispersion of pollutants originated from buoyant sources. An overview of the modelling system is presented in the following. For a more detailed description of the mathematical model, the reader is referred to Kukkonen et al. (2014) and in case of the atmospheric dispersion after the plume rise regime, to Nikmo et al. (1999).

https://doi.org/10.5194/gmd-2021-88
Preprint. Discussion started: 25 May 2021


Geoscientific Model Development Discussions

120

The relevant flow regimes and an overview of the currently applicable modelling system have been presented in Figs. 1a-b. The model includes treatments (i) for the initial plume properties immediately above the fire (source term), (ii) for the dispersion of the buoyant plume and (iii) for the dispersion after the plume rise regime. All of these sub-models constitute a model called BUOYANT. The model can be

125 used to predict the spatial concentration distributions of pollutants originated from fires.

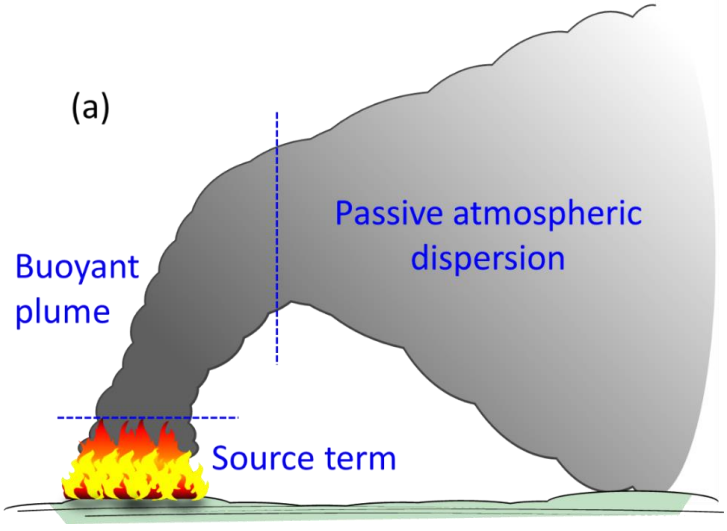

https://doi.org/10.5194/gmd-2021-88
Preprint. Discussion started: 25 May 2021


Geoscientific Model Development Discussions

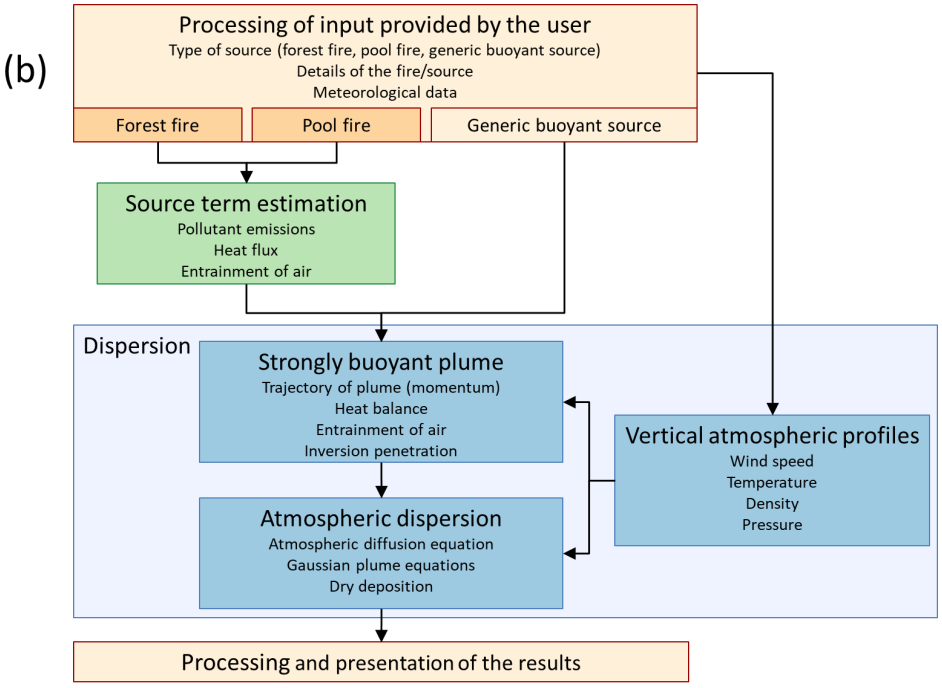


**Figure 1. (a) A schematic presentation of the flow regimes of the dispersion of a fire plume. (b) A block diagram of the BUOYANT model.**

The BUOYANT modelling system also includes an atmospheric dispersion module, which applies the gradient transfer theory and Gaussian equations in the vertical and horizontal directions, respectively (Nikmo et al., 1999). The source strength and the atmospheric conditions are assumed to remain constant in time during the atmospheric dispersion. However, after the plume rise regime, the plume properties can also be used as input information for any other dispersion model.

The plume rise predictions of the BUOYANT model have previously been evaluated against two experimental field data sets regarding prescribed wild-land fires (Kukkonen et al., 2014). These were the "Smoke, Clouds and Radiation – California" experiment (SCAR-C) in Quinault in the US in 1994 (e.g. Kaufman et al., 1996; Gassó and Hegg, 1998) and an experiment in Hyytiälä in Finland in 2009 (e.g., Virkkula et al., 2014a and 2014b). The plume rise treatment of the BUOYANT model has also been evaluated against wind tunnel experiments (Martin et al., 1997; Kukkonen et al., 2000). The dispersion module (after the plume rise regime) has also been tested against the Kincaid field trials (Olesen, 1995; Nikmo et al., 1999). Sofiev et al. (2012) has compared the BUOYANT plume rise predictions against

https://doi.org/10.5194/gmd-2021-88
Preprint. Discussion started: 25 May 2021


the results of the Multi-angle Imaging SpectroRadiometer (MISR) Plume Height Project (e.g., Kahn et al., 2008). In all of the above mentioned model evaluation studies, the model predictions have agreed well or fairly well with the observations.

The plume rise and dispersion treatments of the model contain three physical parameters, the values of which have been determined based on a comparison of model predictions and wind tunnel observations (Kukkonen et al., 2000). The values of these parameters have not been changed or adjusted in any way after their initial determination. The model equations therefore do not contain free parameters that could be adjusted according to the measured values.

### 2.2 The source term model

The source term model can be used to evaluate the characteristics of the plume generated by a fire, which will be needed for the subsequent computations on the evolution of a buoyant plume. The source term model includes treatments to evaluate the properties of a fire plume just above the flame tips, based on information on the characteristics of the fire. The model has been designed to be used also for operational purposes; we have therefore tried to keep the amount and nature of the input data as limited and simple as possible.

The current model version can be applied for two significant categories of fires, viz. the forest and liquid pool fires. In case of forest fires, the input data of the source term model has been selected to include (i) the area of the forest on fire, (ii) the number of trunks per unit area of forest, (iii) the average height of trees and (iv) the average bole diameter at breast height. The input data in case of liquid pool fires includes (i) the burning substance, and (ii) the surface area of the liquid pool on fire. The results of the source term model include (i) the mass fluxes of gaseous and particulate matter produced by a fire, the mass flux of entrained air, and (ii) the characteristic scales of radius, temperature and vertical velocity of the plume.

The source term model does not include an evaluation of the propagation of the actual fire in the terrain; separate models have been developed for this purpose in other studies. The influence of the wind also has not been included in the source term dispersion regime. In case of intensive fires under prevailing light or moderate wind speeds, this is a reasonable assumption. In case of very high wind speeds, allowing

https://doi.org/10.5194/gmd-2021-88
Preprint. Discussion started: 25 May 2021


Geoscientific Model Development Discussions

for the influence of the wind would increase the dilution of the source term, compared with the present computations. However, the influence of the vertical wind structure in the atmosphere has been allowed for in the treatment of the buoyant plume and naturally, in the subsequent atmospheric dispersion (Kukkonen et al., 2014). The fire is assumed to be in the flaming stage; that is the fire burning regime that produces the highest atmospheric concentrations of pollutants.

In the following, we will first address the modelling of (i) the heat fluxes generated by fires and (ii) the average heights of the flames. These results will subsequently be used for deriving equations for (iii) the radius, velocity, temperature and molar flux of a fire plume.

### 2.2.1 Heat fluxes generated by fires

The heat energy of a fire is mostly convected or radiated from the fire region (e.g., Heskestad, 1984 and 2016). A smaller fraction of the heat will also be conducted into the ground (e.g., Ichoku and Kaufman, 2005; Freeborn et al., 2008; Ichoku et al., 2012). The so-called theoretical heat release rate (i.e., heat energy flux) from the fire can be defined to occur, if the burning material is completely combusted. The theoretical heat release rate ($Q$) can be evaluated as (Heskestad, 2016)

$$Q = q_{m,f} H_c, \tag{1}$$

where $q_{m,f}$ is the mass burning rate (i.e., rate of mass burned per time); and $H_c$ is the lower heat of complete combustion (heat energy per burned mass). The lower heat of combustion refers to a situation, in which the fire products are in the state, in which they have been formed (e.g., Drysdale, 2016), i.e., the potential subsequent phase transitions and chemical reactions have not been taken into account. For instance, in this situation any liquid water in the fuel that has been vaporized during the burning process is assumed to be in vapour form. The possible condensation of water therefore does not by definition contribute to the heat released by the fire.

The combustion efficiency $\chi$ is defined as the ratio of the total to the theoretical heat release rate. This efficiency has been found to be close to unity for some fire sources (e.g., methanol and heptane pools), but it may deviate significantly from unity for others (Heskestad, 2016). However, as this efficiency is

https://doi.org/10.5194/gmd-2021-88
Preprint. Discussion started: 25 May 2021


Geoscientific Model Development Discussions

not commonly known in operational applications, we have assumed for simplicity a complete combustion ($\chi = 1$).

The heat flux generated by a fire ($Q$) is propagated in the form of convection ($Q_c$), radiation ($Q_r$) and by other ($Q_o$) means (e.g., conduction),

$$Q = Q_c + Q_r + Q_o \equiv \varepsilon_c Q + \varepsilon_r Q + \varepsilon_o Q, \quad (2)$$

where $\varepsilon_c$, $\varepsilon_r$ and $\varepsilon_o$ are the fractions of convective, radiative and other heat fluxes of the total heat flux $Q$, respectively (by definition, $\varepsilon_c + \varepsilon_r + \varepsilon_o = 1$). Laboratory experiments on biomass burning have demonstrated values of $\varepsilon_o \sim 0.35$ (Freeborn et al., 2008). For large fires, the radiative fraction $\varepsilon_r$ tends to decrease with the increasing size of fire (Heskestad, 2016).

The convective heat flux $Q_c$ can be written simply as (e.g., Achtemeier et al., 2012; Kukkonen et al., 2014; Heskestad, 2016)

$$Q_c = c_p \rho u \pi r^2 \Delta T, \quad (3)$$

where $c_p$ is the specific heat capacity of the plume, $\rho$ is the density of the plume, $u$ is the characteristic velocity of the plume, $r$ is the characteristic radius of the plume and $\Delta T = T - T_a$ is the excess temperature of the plume. $T$ is the characteristic temperature of the plume and $T_a$ is the temperature of ambient air.

### 2.2.2 Mean flame height

The flame intermittency, $I(z)$, is defined as the fraction of time, during which part of the flame is above the height $z$ (Heskestad, 2016). Clearly, the flame intermittency decreases with height; it is equal to unity at the fire source and vanishes at sufficiently large heights. The mean flame height ($\lambda$) is defined as the altitude, at which the flame intermittency has declined to a half of its initial value. At the height $\lambda$, most of the combustion reactions have taken place, and at higher altitudes, the plume can therefore be considered to be inert with a fairly good accuracy (Heskestad, 2016).

https://doi.org/10.5194/gmd-2021-88
Preprint. Discussion started: 25 May 2021


Geoscientific Model Development Discussions

Several experimentally derived correlations have been proposed for $\lambda$. As would physically be expected, $\lambda$ has been found to correlate positively with the fire Froude number, i.e., dimensionless heat release rate $Q^*$ and the pool diameter $d$; which can be written as $\lambda \sim d\ Q^*$ (e.g., Luketa and Blanchat, 2015). In general, Froude number is a dimensionless number defined as the ratio of the flow inertia to the external field; in many applications the external field is gravity. Grove and Quintiere (2002), Dupuy et al. (2003), Luketa and Blanchat (2015) and Heskestad (2016) have presented comparisons of several of the correlations for $\lambda$ in terms of experimental data and against each other.

In this study, we have adopted the correlations of $\lambda$ presented by Zukoski et al. (1985). These correlations performed amongst the best ones in a comparison of predictions and experimental data in large-scale liquid natural gas (LNG) burner experiments that were reported by Luketa and Blanchat (2015). The correlations of Zukoski et al. (1985) also provided physically sensible results in conceivable fire scenarios. These correlations can be written as

$$\lambda = 3.30 d\, Q^{*2/3}, \text{ if } \quad Q^* < 1, \qquad \lambda = 3.30 d\, Q^{*2/5}, \text{ if } \quad Q^* \geq 1, \tag{4a-b}$$

where $d$ is the diameter of a fire source or an equivalent diameter for a noncircular fire with the same area, and $Q^*$ is the Froude number of the fire, defined here as

$$Q^* = \frac{Q}{\rho_a c_{pa} T_a (gd)^{1/2} d^2}, \tag{5}$$

where $\rho_a$ is the density of ambient air, $c_{pa}$ is the specific heat capacity of air at constant pressure and $g$ is the acceleration due to gravity. According to Eq. (5), Froude number is large ($Q^* \gg 1$) for fires, in which the energy output is relatively large compared to its physical diameter.

### 2.2.3 Radius, velocity, temperature and molar flux of a fire plume

The source term model presented in this study is based on the buoyant plume model, which is commonly called the Morton-Taylor-Turner model (Morton et al., 1956; hereafter referred to as MTT). The MTT model is applicable for a steady plume of buoyant material that rises vertically in a calm atmosphere.

https://doi.org/10.5194/gmd-2021-88
Preprint. Discussion started: 25 May 2021


Geoscientific Model Development Discussions

The MTT model applies to sources that have a relatively small difference in density compared to ambient air density (Boussinesq approximation), or to a region above the source, in which air entrainment has brought the plume density sufficiently close to the ambient value.

The coupled first-order differential equations of the MTT model govern the evolution of the characteristic plume radius ($r$), velocity ($u$) and density deficit ($\Delta\rho = \rho_a - \rho$) above a point source. For readability, we have presented these equations and their mathematical solution in Appendix A.

As shown in Appendix A, the solution of these equations can be written in terms of the convective heat flux $Q_c$ (e.g., Heskestad, 1998 and 2016),

$$r = \frac{6\alpha}{5} z, \tag{6a}$$

$$u = \frac{5}{6}\left(\frac{9}{10\pi\alpha^2}\right)^{1/3} g^{1/3}\left(c_p \rho_a T_a\right)^{-1/3} Q_c^{1/3} z^{-1/3}, \tag{6b}$$

$$\frac{\Delta\rho}{\rho_a} = \frac{5}{6}\left(\frac{9\pi^2\alpha^4}{10}\right)^{-1/3} g^{-1/3}\left(c_p \rho_a T_a\right)^{-2/3} Q_c^{2/3} z^{-5/3}, \tag{6c}$$

where $\alpha$ is a dimensionless entrainment coefficient.

The entrainment assumption of the MTT model states that the velocity of entrained air across the plume edge ($u_e$) is proportional to the plume velocity

$$u_e = \alpha u. \tag{7a}$$

However, there are many instances, in which plumes can not be modelled according to the Boussinesq approximation. Observations indicate that in the non-Boussinesq case, the entrainment velocity depends on the ratio of the plume density and the ambient density (Ricou and Spalding, 1961). Morton (1965) suggested, based on experimental evidence and theoretical considerations, an additional proportionality of the entrainment velocity,

https://doi.org/10.5194/gmd-2021-88
Preprint. Discussion started: 25 May 2021


Geoscientific Model Development Discussions

$$u_e = \alpha \left(\frac{\rho}{\rho_a}\right)^{1/2} u, \tag{7b}$$

which is usually referred to as the Ricou-Spalding entrainment model; hereafter referred to as RS. Equation (7b) indicates a reduced entrainment into lighter plumes, in comparison with entrainment to plumes of near ambient air density.

For extending the model to other than point sources, a concept of virtual source can be introduced. The virtual source is located below the actual area source and is accounted for by replacing the height $z$ by $z - z_{vs}$, where $z_{vs}$ is the height of the virtual source. In addition, to accommodate large density deficiencies, Morton's extension of the MTT model results in that the plume radius in the right-hand side of Eq. (6a) has to be multiplied by a factor $(\rho_a/\rho)^{1/2}$ and the ratio $\Delta\rho/\rho_a$ in Eq. (6c) has to be replaced by $\Delta\rho/\rho$ (Morton, 1965).

The comparison of model predictions and measurements of fire plumes above the flames have to a large extent supported the use of the above described theory (Heskestad, 1984 and 1998). However, the prediction accuracy can be improved by using experimentally adjustable coefficients. The plume radius ($r_{\Delta T}$), and the mean values of velocity ($u_0$) and excess temperature ($\Delta T_0 = T_0 - T_a$) at the plume centre line have been found to obey the following relations (Heskestad, 1984 and 1998):

$$r_{\Delta T} = C_1 \left(\frac{T_0}{T_a}\right)^{1/2} (z - z_{vs}), \tag{8a}$$

$$u_0 = C_2 \left(\frac{g}{c_p \rho_a T_a}\right)^{1/3} Q_c^{1/3} (z - z_{vs})^{-1/3}, \tag{8b}$$

$$\Delta T_0 = C_3 \left(\frac{T_a}{g c_p^2 \rho_a^2}\right)^{1/3} Q_c^{2/3} (z - z_{vs})^{-5/3}, \tag{8c}$$

where $r_{\Delta T}$ is the plume radius at the point where the excess temperature is $0.5\Delta T_0$, $T_0$ is the mean temperature in the centre line of the plume, and $C_1 = 0.12$, $C_2 = 3.4$ and $C_3 = 9.1$ are experimental coefficients. The above values of the coefficients $C_i$ ($i = 1,3$) are based on experimental investigations of heated air jets and large-scale pool fires (George Jr. et al., 1977; Kung and Stavrianidis, 1982). For burn

https://doi.org/10.5194/gmd-2021-88
Preprint. Discussion started: 25 May 2021


Geoscientific Model Development Discussions

experiments in rack storage fires, Kung et al. (1988) and Tamanini (2010) have recommended slightly different values of $C_i$ ($i$ = 1,3).

For fire sources, which do not have substantial in-depth combustion, the height of the virtual source $z_{vs}$ can be estimated based on the experimental relation of Heskestad (1984),

$$z_{vs} = -1.02d + 0.083\left(\frac{Q}{1000}\right)^{2/5}. \quad (9)$$

A fire source does not have substantial in-depth combustion, if a major fraction of the volatiles released (2/3 or higher) undergoes combustion above the fuel array (Heskestad, 1984). Fire sources with substantial in-depth combustion include, e.g., very openly constructed, or well-ventilated wood cribs.

Assuming ideal gas behaviour, the molar flux of gaseous material ($q_n$) of the plume is

$$q_n = \frac{p_a}{R_g T}\pi r^2 u, \quad (10)$$

where $p_a$ is the atmospheric pressure (pressure within the plume is assumed to be equal to the ambient value) and $R_g$ is the molar gas constant. The flux $q_n$ comprises of the molar fluxes of air ($q_{n,a}$) and gaseous combustion products ($q_{n,c}$),

$$q_n = q_{n,a} + q_{n,c}. \quad (11)$$

Detailed modelling of the two selected application areas has been presented in Appendix C.

### 2.2.4 Interface of the source term and plume rise regimes

The mean velocity ($u_0$) and excess temperature ($\Delta T_0$) in Eqs. (8b-c) are values at the centre line of a fire plume. As the radial distance from the centre line increases, $u$ and $\Delta T$ approach their ambient values. We have assumed Gaussian distributions for the radial distributions of velocity and temperature in the source term regime.

https://doi.org/10.5194/gmd-2021-88
Preprint. Discussion started: 25 May 2021


Geoscientific Model Development Discussions

However, the subsequent modelling phase in the plume rise regime assumes that the plume is described by a uniform (top-hat) distribution of physical quantities. If the centre line values of the Gaussian distributions ($u_0$, $\Delta T_0$) would be used to represent a top hat profile, the convective heat would not in general be conserved at the boundary of the source term model and the plume rise model.

We have therefore presented a solution in Appendix B, in which the convective heat is conserved at the boundary of the two modelling regimes. According to this solution, the top hat velocity ($u$) and excess temperature ($\Delta T$) in the plume rise regime are related to the values at the centre line of the Gaussian plume in the source terms regime as follows (utilizing the values of the coefficients $C_i$ ($i$ = 1,3) presented in Eqs. (8a-c)):

$$u = 0.86u_0, \quad (12a)$$

$$\Delta T = 0.83\Delta T_0. \quad (12b)$$

The model is not applicable for $\pi C_1^2 C_2 C_3 < 1$, as required by the conservation of heat energy, as presented in detail in Appendix B.

Detailed modelling of the fluxes of compounds originated from the two selected fire types have been presented in Appendix C.

#### 2.2.5 Summary of the use of the model equations and the computer model

For both types of fires, mean flame height is evaluated from Eqs. (4a-b). The initial plume radius, vertical centre line velocity, and the excess temperature of the plume are evaluated from Eqs. (8a-c). The mass flux of entrained air is computed applying Eqs. (9-11).

In case of a forest fire, the convective heat flux and the mass fluxes of pollutants originating from a fire are computed based on Eqs. (1), (C6) and (C7), and applying the emission factors presented by Kaiser et al. (2012). In case of a pool fire, the convective heat flux and the mass fluxes of pollutants originating from a fire are evaluated based on Eqs. (1), (3), (C1) and (C2). In addition, the model applies for pool fires the fuel property data presented in Table C1. The velocity and temperature required for the subsequent plume rise regime are computed based on Eqs. (12a-b).

https://doi.org/10.5194/gmd-2021-88
Preprint. Discussion started: 25 May 2021


Geoscientific Model Development Discussions

## 3 Evaluation of the model against experimental data

### 3.1 Overview of the RxCADRE experiments

We have evaluated the model against the experimental data of the Prescribed Fire Combustion and Atmospheric Dynamics Research Experiment, RxCADRE. The experiments were designed to collect extensive data before, during and after the active burning periods of prescribed fires. These datasets are one of the most comprehensive field campaigns to date, providing accurate measurements of various aspects of the fires, including meteorology, the evolution of fires, their energy, the emissions and airborne concentrations (Ottmar et al., 2016a; Clements et al., 2019; Prichard et al., 2019).

The RxCADRE experiments were conducted in Florida, USA during 2008–2012. These datasets have previously been used, for instance, in the evaluation of the empirical-stochastic plume model Daysmoke (Achtemeier et al., 2012), the Stochastic Time-Inverted Lagrangian Transport (STILT) model (Mallia et al., 2018), and the Weather Research and Forecasting Model combined with a semi-empirical fire-spread algorithm (WRF-SFIRE) (Mallia et al., 2020; Moisseeva and Stull, 2019).

For readability, we present a brief description of the experiments and measured data, which were used in this study. For a more detailed description of the experiments, the reader is referred to a special issue of the International Journal of Wildland Fire, which was aimed to document the RxCADRE study (Peterson and Hardy, 2016). In particular, Ottmar et al. (2016a and 2016b) has presented overviews of the RxCADRE study.

The RxCADRE measurement campaign consisted of six smaller (less than 10 ha) and ten larger (10 - 900 ha) prescribed fires (Ottmar et al., 2016a). Measured data that is sufficient for dispersion model evaluation is available for three larger fires: two grass fires (named by the authors as L1G and L2G, in which L presumably refers to larger experiments and G to grass) and one sub-canopy forest fire (named as L2F, in which F refers to forest) (Clements et al., 2016; Dickinson et al., 2016; Strand et al., 2016). In case of these three experiments, data is available regarding the meteorological conditions, fire emissions and airborne concentrations.

https://doi.org/10.5194/gmd-2021-88
Preprint. Discussion started: 25 May 2021


As the main focus of the present study was on forest fires, we have selected the L2F fire for model evaluation. This experiment was conducted over a burn block of size 151 ha at Eglin Air Force Base, Florida. The L2F burn experiment was conducted on 11 November 2012, from 18 to 22 UTC. The amount of burned organic material was approximately 4.13 Mg ha$^{-1}$ (Ottmar et al., 2016b). Approximately 65 % of the burned material consisted of litter, 21 % of down-and-dead fine wood (≤ 7.6 cm in diameter), 13 % of shrub, and about 1 % of herbaceous plants (grasses and forbs). The experimental data is publicly available in the Research Data Archive of United States Department of Agriculture (RDA, 2018). The dataset includes aircraft concentration measurements of CO, $CO_2$, $CH_4$ and $H_2O$ (Urbanski, 2014b; Strand et al., 2016). However, there were neither aircraft measurements on particulate matter nor ground-based measurements in the publicly available dataset. We have therefore conducted the model evaluation using the concentration data on gaseous substances from aircraft measurements in the experiment L2F.

The accuracy of the meteorological measurements within the L2F burn was evaluated by Seto and Clements (2015a and 2015b). They concluded that the data are qualitatively reliable. Urbanski (2014b) analyzed the accuracy of the airborne concentrations, regarding the positioning by GPS and the applied spectroscopic methods (Cavity ring-down spectroscopy, CRDS). The estimated analytical uncertainty of the CRDS measurements varied from 1 % to 1.5 % for $CO_2$ and $CH_4$, and from 2 % to 15 % for CO.

### 3.2 The selected experiment, the sub-canopy forest fire (L2F)

The radiative heat fluxes of the fire were evaluated using long-wave infrared (LWIR) measurements (Dickinson et al., 2016). The measurements were done onboard a twin-engine Piper Navajo aircraft, which was used to make repeated passes at about three-minute intervals (Dickinson et al., 2016).

The aircraft measurements yielded data of fresh emissions, vertical profile of the smoke, plume height and the dispersion of smoke (Urbanski, 2014b). Measurements were conducted at distances of up to 25 kilometres downwind from the source. Measurements were done as so-called parking garage and corkscrew flight profiles. Parking garage vertical profiles involved short (approximately 10 km) horizontal transects, roughly perpendicular to the axis of the smoke plume, taken at multiple elevations. Corkscrew profiles were centered on the plume downwind from the burn unit. Parking garage and

https://doi.org/10.5194/gmd-2021-88
Preprint. Discussion started: 25 May 2021




corkscrew manoeuvres were designed for measuring the horizontal and vertical concentration distributions, respectively.

The observations of the heat fluxes were used for deriving the fire radiative power (FRP) against time. The evaluated temporal evolutions of the FRP and the burning area are presented in Fig. 2.

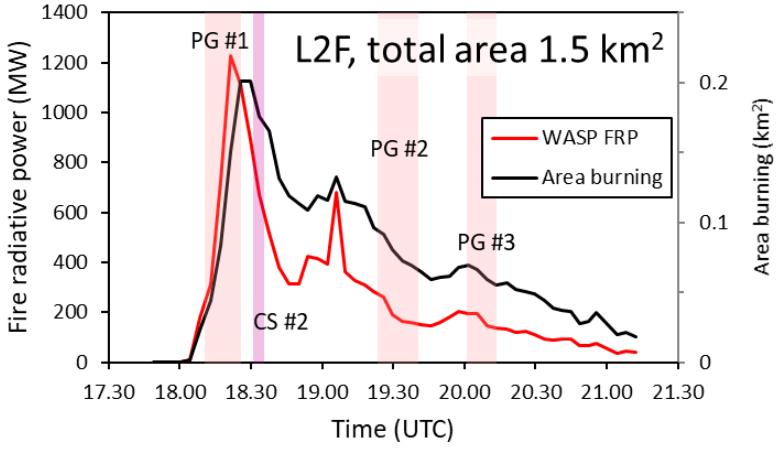


**Figure 2. Evaluated temporal evolutions of the fire radiative power (FRP) (red curve, left-hand vertical axis) and the active fire area (black curve, right-hand vertical axis) of the L2F burn. The FRP values were taken from the data presented by Hudak et al. (2016a). WASP refers to Wildfire Airborne Sensor Program. Transects of the measurement aircraft are denoted by four light red or violet coloured vertical bars (PG #1, CS #2, PG #2 and PG #3); data extracted from Urbanski (2014b). PG and CS refer to the parking garage and corkscrew flight manoeuvres, of the measurement aircraft, respectively.**

We have compiled Fig. 2 based on the data presented by Hudak et al. (2016a) and Urbanski (2014b). The figure illustrates that there were substantial temporal changes of the fire during the experiment, both regarding the intensity of the fire and its spatial extent. The timing of the aircraft flights focuses on one hand on the most intensive periods of the fire (PG #1 and CS #2), on the other hand on covering the whole period of the fire (PG #2 and PG #3). The flight CS #1 was done before the ignition of the fire.

The measured airborne concentrations represented average values of 2 seconds; these are included in the available dataset. However, we have computed and applied observed concentrations as 20 second centered moving averages, in agreement with Mallia et al. (2018).

https://doi.org/10.5194/gmd-2021-88
Preprint. Discussion started: 25 May 2021


Geoscientific Model Development Discussions

### 3.3 Evaluation of meteorological variables and the fire source

#### 3.3.1 Evaluation of the meteorological variables

The vertical profiles of wind speed, temperature and pressure required by the model were determined by applying the onsite measurements (Clements et al., 2016). The meteorological measurement campaign of RxCADRE consisted of a variety of measurement platforms and instrument types. We have applied the data collected by the California State University - Mobile Atmospheric Profiling System (CSU-MAPS) for the evaluation of atmospheric properties. For evaluations near the ground surface (up to a height of 30 m), we used measurements in the micrometeorological mobile tower, which was located downwind of the L2F burn plot. Above the height of 30 m, Doppler lidar measurements were used. The lidar was placed on the perimeter of the L2F burn unit.

We applied the meteorological measurements prior to the ignition of the L2F burn. Ten-minute averages of measured wind speed, wind direction, ambient temperature and ground level air pressure were applied for further processing. The Monin-Obukhov length ($L$) was estimated by fitting the atmospheric vertical profiles used in the BUOYANT model (Kukkonen et al., 2014) to the averaged temperature and wind measurements, using the method presented by Nieuwstadt (1978). The two-layered thermal structure above the atmospheric boundary layer (ABL) was evaluated by applying the measured temperature profile, according to the method by Fochesatto (2015).

Prevailing wind direction was evaluated to be south-easterly at 132°. The modelled wind speed and ambient temperature at the altitude of 10 m were evaluated to be 3.2 m $s^{-1}$ and 24 °C, respectively. The atmospheric stability was estimated to be moderately stable ($L^{-1}$ = 0.0011 $m^{-1}$). Based on the observed temperature profile, the height of the ABL was estimated to be 2.2 km. The gradients of potential temperature were estimated to be 0.0193 K $m^{-1}$ and 0.0094 K $m^{-1}$ within the inversion and upper layers, respectively. Wind speed above the ABL was assumed to be constant and equal to the modelled value at the top of the ABL, 14 m $s^{-1}$.

#### 3.3.2 Evaluation of the properties of the fire source

The properties of the fire source term could in principle be evaluated using the source term model that has been presented in this article. However, for this particular measurement campaign, it is better to use directly the values that were reported in the database and the relevant publications regarding the

https://doi.org/10.5194/gmd-2021-88
Preprint. Discussion started: 25 May 2021




experiment. The source term model presented in section 2.2. was therefore not applied in the following evaluation exercise. Instead, the evaluation has been made for the BUOYANT model, by selecting the option of not using the fire source term module.

We have assumed a steady state of the fire in the modelling, as the model is not capable of treating time-dependent releases. The following properties of the fire source need to be known as input values for executing the BUOYANT model: (i) fire radiative power (FRP), (ii) the convective fraction of energy release from the fire ($\varepsilon_c$), (iii) the physical extent of the fire ($a_f$), (iv) the temperature of fire products ($T_f$), and (v) the mass fluxes of the fire products ($q_f$).

For evaluating the properties from (i) to (iv), we have applied the observed values as reported by Hudak et al. (2016a) and Jimenez and Butler (2016), averaged over the measurement period. Time-averaged mass flux (v) of $CO_2$ was derived from the experimentally determined fuel consumption and emission factors (Hudak et al., 2016b; Strand et al., 2016). The averaged values of the fire source applied for the dispersion computations were: FRP = 283 MW, $\varepsilon_c$ = 0.324, $a_f$ = 0.079 km$^2$, $T_f$ = 58 °C, and $q_f$ = 113 kg s$^{-1}$ (the mass flux of $CO_2$).

### 3.4 Results of the model evaluation

We consider in the following observed and modelled excess concentrations, i.e., concentrations subtracted by background concentration. These represent the contributions of the fire. We focus on the comparison of the measured and predicted spatial concentration distributions, in the horizontal and vertical directions. The aircraft measurements were specifically designed to measure such distributions.

The model does not contain any free parameters and was not adjusted in any way to the measured data.

Measured and modelled vertical excess concentrations of $CO_2$ are presented in Fig. 3, for three parking garage and the second corkscrew flight paths. The flight durations varied from 6 (PG #1) to 16 minutes (PG #2).

https://doi.org/10.5194/gmd-2021-88
Preprint. Discussion started: 25 May 2021


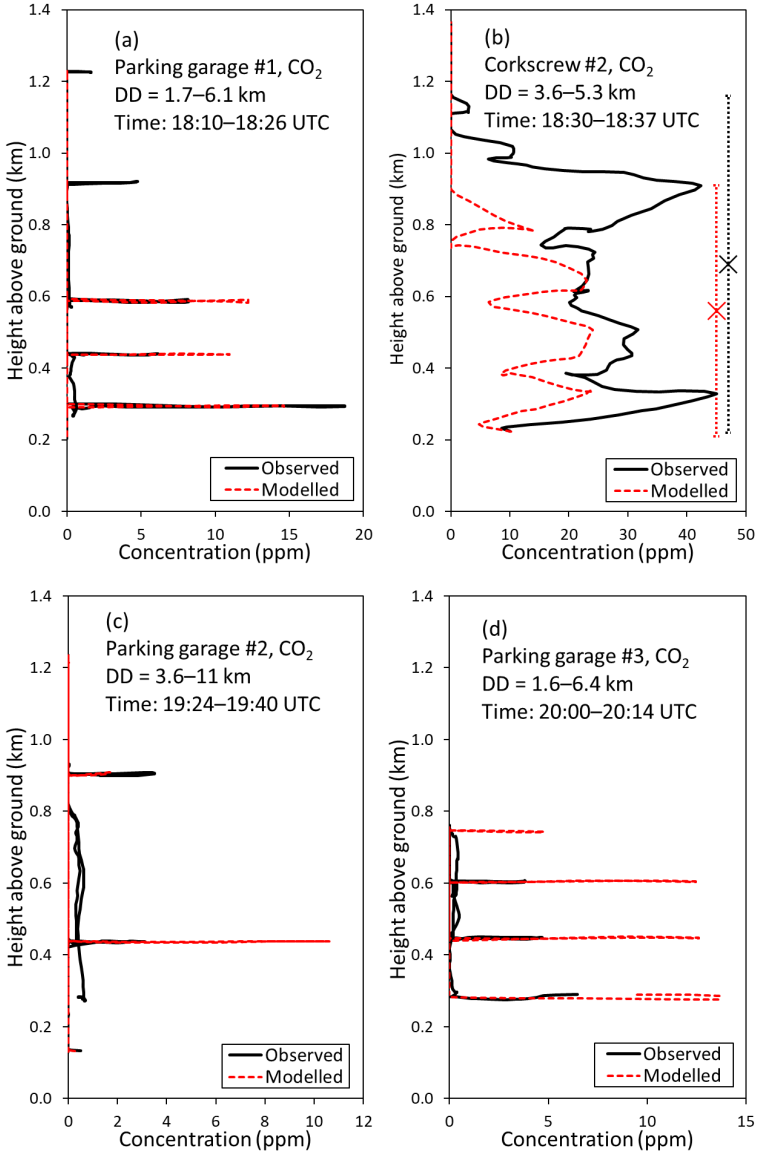


500 **Figure 3. Observed (in black) and modelled (in red) vertical excess concentrations of $CO_2$ for three parking garage and the second corkscrew flight manoeuvres. In Fig. 3b, the observed and modelled vertical extents of plume have also been shown as vertical bars on the right-hand side of that panel. The centre points of the vertical extents of plume are marked with cross-hairs. Notation: DD = the downwind distance from the centre of the L2F burn block, time = the time interval of the manoeuvre of the measurement aircraft, UTC = Coordinated Universal Time.**

505

The observed vertical excess concentration distributions of $CO_2$ during the parking garage manoeuvres are temporally well captured by the model, for most of the highest concentrations (Figs. 3a, c and d).

https://doi.org/10.5194/gmd-2021-88
Preprint. Discussion started: 25 May 2021


Geoscientific Model Development Discussions

However, there are both over- and underpredictions of the highest measured concentrations. For instance, regarding the parking garage flight #1, the highest measured peak concentration is underpredicted, whereas the second and third highest measured concentrations are overpredicted. For the parking garage flight #3, the magnitudes of all the highest peaks are overpredicted.

The modelled extent of the plume in the vertical direction (700 m) is smaller than indicated by the measurements (940 m), as shown in Fig. 3b. The model also estimates the plume to be at slightly lower elevation compared to the observations: modelled centre of the distribution is at about 560 m, while measurements indicate an elevation of 690 m.

Measured and modelled horizontal excess concentrations of $CO_2$ during the three parking garage flight paths are shown in Fig. 4. The model predictions compare fairly well with the observations. Concentration peaks tend to be overestimated by the model (also seen in Fig. 3), while the widths of the plume are slightly underestimated.

https://doi.org/10.5194/gmd-2021-88
Preprint. Discussion started: 25 May 2021


Geoscientific Model Development Discussions
Open Access
EGU

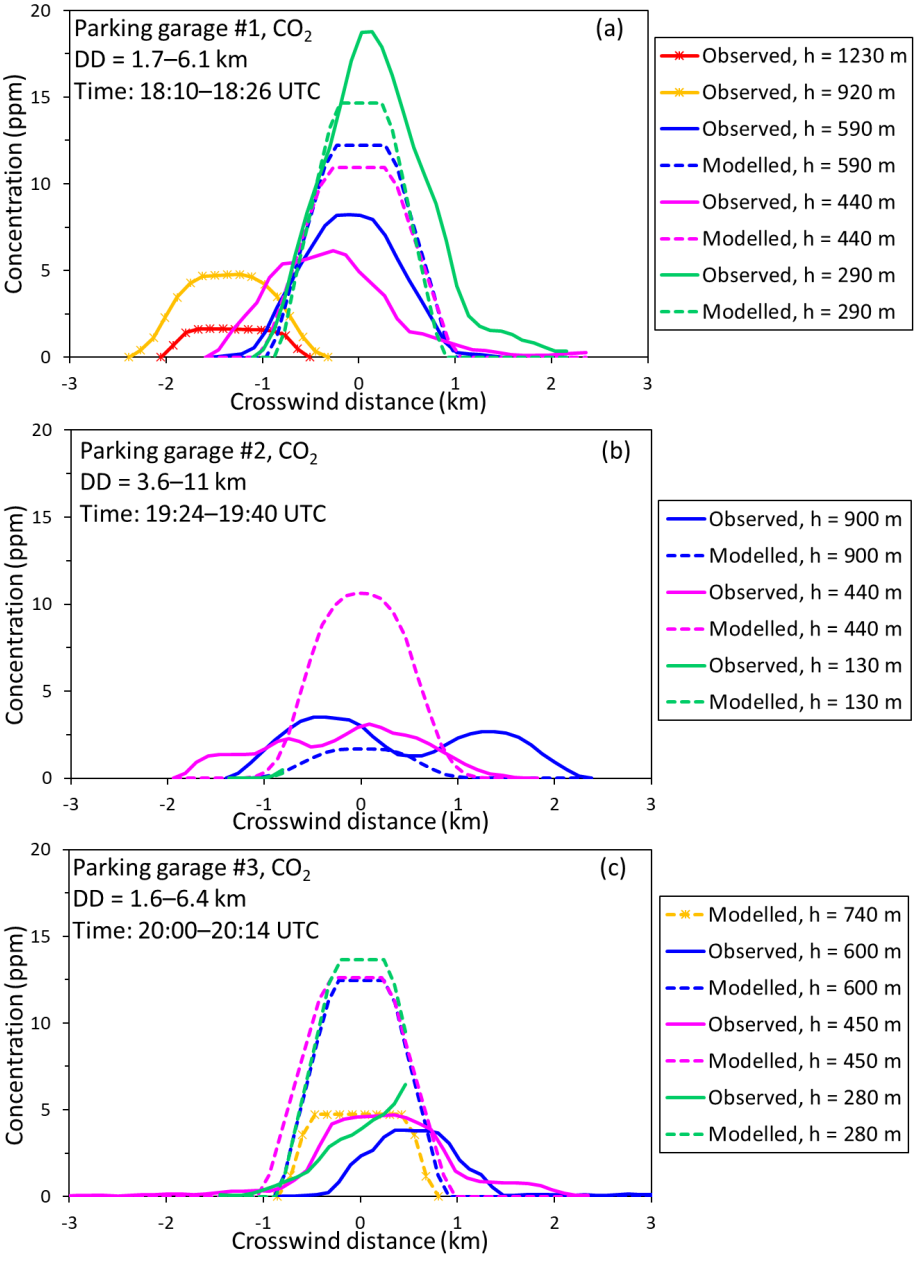


525 **Figure 4. Observed (solid lines) and modelled (dashed lines) horizontal excess concentration distributions of $CO_2$ for three parking garage flight manoeuvres. Notation: DD = downwind distance from the centre of the L2F burn block, time = the time interval of the manoeuvre of the measurement aircraft, *h* = the elevation above ground, UTC = Coordinated Universal Time.**

https://doi.org/10.5194/gmd-2021-88
Preprint. Discussion started: 25 May 2021


There are several reasons for the differences of the measured and predicted concentrations. In particular, there are several challenges in determining the source properties and the meteorological conditions in such field experiments.

First, the modelling assumed a steady state of the fire. This implies that the fire intensity was assumed to be temporally constant throughout the whole duration of the experiment. The model therefore tends to underpredict the concentrations in the initial stages of the fire (PG #1 and CS #2) and overpredict these in the later stages (PG #2 and #3). However, the temporal agreement of the measured and modelled highest concentrations was good.

For the modelling of fire plumes, it is crucial to evaluate sufficiently accurately the vertical structure of the atmosphere, especially the potentially existing temperature inversions. Kukkonen et al. (2014) previously compared the predictions of the BUOYANT model against the measurements in two other field measurement campaigns. They commented that, e.g., evaluating the meteorological conditions in the SCAR-C experiments (Kaufman et al., 1996; Hobbs et al., 1996; Gassó and Hegg, 1998) using two different meteorological methods, resulted in substantially different meteorological input data values for the model.

In case of the RxCADRE measurements, the relevant meteorological parameters have been carefully measured and well reported. However, the application of such datasets in determining vertical atmospheric profiles of the relevant quantities, and the atmospheric stability conditions, will result in some degree of inaccuracy in the dispersion modelling.

## 4 The operational version of the model

We have compiled an operational version of the model. The main aim of developing this version was to provide a user-friendly tool of assessment for various emergency response personnel. The operational model can be used for emergency contingency planning and for the training of emergency personnel, in case of forest and pool fires.

https://doi.org/10.5194/gmd-2021-88
Preprint. Discussion started: 25 May 2021


Geoscientific Model Development Discussions

555 ### 4.1 Overview and functioning of the operational model

The operational program has been named as FLARE (Fire pLume model for Atmospheric concentrations, plume Rise and Emissions). An overview of the model structure has been presented in Fig. 5. This model contains the program BUOYANT for conducting the physical and chemical computations, a graphical user interface, and various modules for processing the input and output data of the model. The operational
560 version can be used remotely via an internet connection.

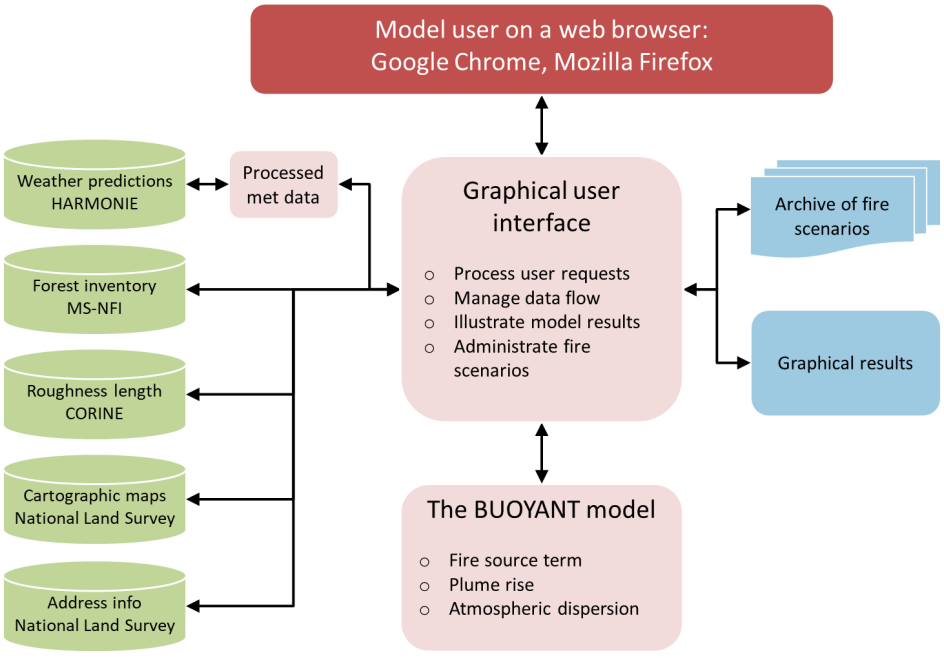


565 **Figure 5. Block diagram of the operational model. The red, green, light red and blue colours indicate the internet connections, the data sources, the main model components and the output components, respectively. The arrows indicate the flow of data. Acronyms: MS-NFI = Finnish Multi-Source National Forest Inventory, CORINE = CoORrdination of INformation on the Environment.**

The graphical user interface is used for processing the input data by the model user, managing of the flow of data within the operational model, illustrating the numerical results and administrating the
570 archived fire cases. The navigation through the model input screens has been designed to be as user-friendly and straightforward as possible. The program can be used with the latest versions of the web browsers, which are most frequent used; the recommended browsers are Google Chrome and Mozilla Firefox.

https://doi.org/10.5194/gmd-2021-88
Preprint. Discussion started: 25 May 2021


575 The model addresses forest fires and liquid pool fires. The user needs to specify as input values only the location and time of the fire event, the estimated area of the fire, and in case of a pool fire, the released substance. In addition, the model pre-processes and provides for the computations three main types of input data: meteorological parameters, forest information and geographic maps.

580 The program will subsequently check that all the user-specified input data values and their combinations are physically reasonable. The program will also check that the computations address cases, which are within the applicability range of the model. In case of unrealistic or unreasonable input values, the program will either request the user to confirm the value or to input a more realistic value.

585 However, the current version of the operational model can be used only for locations that are situated in Finland, or in close vicinity of the country. The operational model could be extended to function also in other countries and regions, by expanding especially the cartographic and forest inventory datasets. In case of missing input datasets, the model could also be modified to skip some of the input processor modules and ask the user to input the corresponding values. For instance, if there would not be a suitable
590 forest inventory available for the considered domain, the user would be asked to supply the required information on the characteristics of the forest.

The user can archive descriptions of fire events, which contain input data for a range of potential fire scenarios. These cases can then be retrieved, edited as necessary, and used for further computation.

595

The program presents the numerical results as pollutant iso-concentration curves on maps. The current operational version presents spatial concentration distributions of carbon dioxide ($CO_2$) near the ground level.

### 4.2 The pre-processing of the input datasets

600 The functioning of the operational model has been made as user-friendly as possible, by an automatic pre-processing of several input materials. The meteorological parameters and forest inventory data will be extracted and preprocessed for the spatial coordinates and the time specified by the model user. The model also presents the results on geographic maps, for the domain selected by the user.

https://doi.org/10.5194/gmd-2021-88
Preprint. Discussion started: 25 May 2021


The automatic on-line use of weather and forest data makes the use of the model substantially quicker and simpler. This will also reduce potential human errors. For non-expert users, the determination of the required meteorological variables would otherwise be a very challenging task. In case of long-term fires, the user can also use the forecasted meteorological values, for forecasting the spread of the fire plumes for up to two days ahead in time.

These input datasets and pre-processors are briefly described in the following. Additional information regarding the meteorological data is presented in Appendix D.

#### 4.2.1 Meteorological data

The program can use either real-time or forecasted meteorological data produced by the numerical weather prediction (NWP) model HARMONIE; this model is run operationally at the FMI. The acronym HARMONIE has been derived from "HIRLAM ALADIN Research on Mesoscale Operational Numerical weather processing In Euro-Mediterranean Partnership" (Nielsen et al., 2014). The modelling domain includes Fennoscandia, the Baltic Countries and the surrounding regions in the eastern Atlantic, Northern Central Europe and Russia.

The HARMONIE model was selected for three main reasons. First, this model has been thoroughly evaluated against experimental data and it is known to provide accurate, high-resolution weather forecasts for the whole of Fennoscandia. The treatments of this model have been specifically adopted for the conditions in the Northern European region. Second, the NWP computations are performed operationally in-house, which simplifies the transfer of data between the operational program and the NWP model. Third, the HARMONIE system will be the operational weather forecasting model in Finland in the near future (replacing the older HIRLAM NWP model).

However, the output data of this NWP model does not directly include all the input values required by the BUOYANT model. We have therefore constructed a continuously functioning pre-processor model, which evaluates the required meteorological parameters based on the output of the HARMONIE model. These parameters are the ambient temperature and pressure, the lateral wind components, the inverse

https://doi.org/10.5194/gmd-2021-88
Preprint. Discussion started: 25 May 2021


Monin-Obukhov length, the height of the atmospheric boundary layer and the vertical profiles of temperature and wind speed above ABL.

The meteorological roughness length, which will be needed in the atmospheric dispersion computations, is evaluated based on the CORINE (CoORrdination of INformation on the Environment) land cover information in 2012, using in addition the weighting coefficients modified by Venäläinen et al. (2017).

### 4.2.2 Forest information

In case of forest fires, the amount of burnt material is evaluated based on a national inventory of forests (Mäkisara et al., 2019). This inventory has been compiled by the Natural Resources Institute Finland, and it is called Multi-Source National Forest Inventory of Finland (MS-NFI). The methods and results of this inventory have been presented by Tomppo and Halme (2004). The inventory is publicly available.

The inventory contains forest resource maps, classified under 44 themes. The inventory has been constructed based on satellite images, field data collected nationally and digital map data. The data covers the whole of Finland and part of the areas in Northern Sweden and Russia. The spatial resolution of the data is 16 m × 16 m.

The model uses the results of this inventory, corresponding to the year 2015. The relevant parameters are the number of trunks per unit area of forest, the average height of trees and the average bole diameter at breast height. The values of these parameters are automatically selected from the inventory, corresponding to the user-specified location and surface area of the fire.

### 4.2.3 Geographic map information

The model provides as output spatial concentration distributions near the ground level, presented on digital maps. The model uses open-access maps provided by the National Land Survey of Finland. The user can specify the location of the accident by simply clicking that point in the map, by specifying the geographic coordinates or by writing the street address. The accident location will then be searched and the coordinates will be extracted from the Finnish National Geoportal (National Land Survey of Finland, 2021). This location will then be automatically placed on a map. For efficient functioning, this service has been adapted to the computer facilities at the Finnish Meteorological Institute (FMI).

https://doi.org/10.5194/gmd-2021-88
Preprint. Discussion started: 25 May 2021


Geoscientific Model Development Discussions

## 5 Conclusions

We have presented a refined version of a mathematical model, BUOYANT, which has been designed for analyzing the formation and dispersion of plumes originating from major fires. The model addresses the cross-plume integrated properties of a rising plume in a vertically varying atmosphere; the model also takes into account the impacts on plume rise of possibly occurring inversion layers (Kukkonen et al., 2014). In the present study, the BUOYANT model has been extended to include a more detailed description of the early development of the fire plume. This generalization also made it possible to compile an operational model version, which can be used in a much more straightforward way, compared with the use of the original research model.

The developed source term model can be used to evaluate the characteristics of the fire plume, which can be used as input for the subsequent computations on the evolution of a buoyant plume. The source term model uses as input the information on the characteristics of the fire, and it is used to evaluate the properties of a fire plume just above the flame tips. The current version of the source term model can be applied for two significant categories of fires, viz. the forest and liquid pool fires. In future work, the source term model could be generalized to address also other fire types. The main model structure of the source term model is based on the differential equations for releases of buoyant material, which govern the evolution of the plume radius, velocity and density difference. However, the model can be considered to be semi-empirical, as it also relies on various experimental results on fire plumes.

We have compared the predictions of the refined BUOYANT model against the experimental field-scale data of the RxCADRE campaign (Prescribed Fire Combustion and Atmospheric Dynamics Research Experiment). These experiments were designed to collect extensive quantitative data regarding the burning of prescribed fires. These datasets have provided accurate measurements of various aspects of the fires, including meteorology, the evolution of fires, their energy, the emissions and airborne concentrations. The predicted concentrations of $CO_2$ agreed fairly well with the aircraft measurements of the RxCADRE campaign. For instance, the model captured well the observed vertical excess concentration distributions of $CO_2$ during the parking garage flight manoeuvres, for most of the highest concentrations. However, the model tended to moderately overpredict the highest concentrations, whereas the widths of the plume were slightly underestimated.

https://doi.org/10.5194/gmd-2021-88
Preprint. Discussion started: 25 May 2021


There are several reasons for the differences of the measured and predicted concentrations. Previous comparisons of the predictions of plume rise models and experimental field-scale data have illustrated several major challenges in determining accurately the source properties and the meteorological conditions (e.g., Kukkonen et al., 2014). These are also major sources of uncertainty in the present comparisons against the RxCADRE data.

An important limitation of the present modelling is that it has assumed a steady state of the fire. This implies that the fire intensity was assumed to be temporally constant throughout the whole duration of the experiment. Clearly, the influenc of this assumption could to some extent be taken into account by conducting several computations with the model, using various values of the fire intensity. The influence of the steady state assumption is that the model tended to underpredict the concentrations in the initial stages of the fire and to overpredict these in the later stages. The model currently assumes that the burned material consists solely of standing tree trunks. Clearly, also other kinds of plant material contribute to the burning in a forest.

Another source of uncertainties in the modelling is the evaluation of the relevant meteorological parameters. The meteorological measurements in the RxCADRE campaign have been carefully measured and reported. However, the application of such data for determining vertical atmospheric profiles of the relevant quantities, and the atmospheric stability conditions, will inherently result in some inaccuracies.

We have also compiled an operational version of the model. The operational model is a user-friendly tool of assessment that can be used by various emergency response and rescue personnel. This model can be used for emergency contingency planning and for the training of emergency personnel, in case of forest and pool fires. The model has been used by Finnish rescue authorities up to date. However, it would be possible to use both the original research model and its operational application also worldwide, the latter after some adjustment of the processing of the model input datasets. This could potentially result in improved preparedness and better, knowledge-based rescue actions in case of major fires.

https://doi.org/10.5194/gmd-2021-88
Preprint. Discussion started: 25 May 2021


Geoscientific Model Development Discussions

## Appendix A. The Morton-Taylor-Turner model for a buoyant plume

Let us consider a plume from a point source, assuming no momentum flux at the source, uniform ambient air density and the Boussinesq approximation. The conservation of mass, momentum and buoyancy can be written as (Morton et al., 1956)

$$\frac{d}{dz}(r^2 u) = 2 r u_e, \quad \text{(volume/mass)}, \tag{A1a}$$

$$\frac{d}{dz}(r^2 u^2) = r^2 g \left(\frac{\rho_a - \rho}{\rho_a}\right), \quad \text{(momentum) and} \tag{A1b}$$

$$\frac{d}{dz}\left(r^2 u g \frac{\rho_a - \rho}{\rho_a}\right) = 0, \quad \text{(buoyancy)}, \tag{A1c}$$

where $z$ is the height above ground; $r$ is the radius of the plume; $u$ is the vertical velocity of the plume; $u_e$ is rate of entrained air across the plume edge (entrainment velocity); $g$ is the acceleration due to gravitation; $\rho_a$ is the density of ambient air; and $\rho$ is the density of the plume.

The entrainment velocity is assumed to be proportional to some characteristic velocity at height $z$ (Morton et al., 1956)

$$u_e = \alpha u, \tag{A2}$$

where $\alpha$ is an experimentally defined proportionality constant (the entrainment constant) relating the entrainment velocity to the vertical velocity within the plume. Equation (A2) is often referred to as the Morton-Taylor-Turner entrainment model.

The solution of Eqs. (A1a-A1c) is (Morton et al., 1956)

$$r = \frac{6\alpha}{5} z, \tag{A3a}$$

$$u = \frac{5}{6\alpha}\left(\frac{9}{10}\alpha B\right)^{1/3} z^{-1/3}, \tag{A3b}$$

https://doi.org/10.5194/gmd-2021-88
Preprint. Discussion started: 25 May 2021


Geoscientific Model Development Discussions

$$g\frac{\rho_a-\rho}{\rho_a}=\frac{5B}{6\alpha}\left(\frac{9}{10}\alpha B\right)^{-1/3}z^{-5/3}, \tag{A3c}$$

where the constant buoyancy flux $B$ is

$$B=r^2ug\frac{\rho_a-\rho}{\rho_a}. \tag{A4}$$

Assuming ideal gas behaviour, the buoyancy flux can be written in terms of convective heat flux ($Q_c$) as (Heskestad, 2016)

$$B=\frac{gQ_c}{\pi c_p T_a \rho_a}. \tag{A5}$$

https://doi.org/10.5194/gmd-2021-88
Preprint. Discussion started: 25 May 2021


Geoscientific Model Development Discussions

## Appendix B. Centre line properties of a fire plume in the source term regime and the equivalent top-hat profiles

The mean velocity ($u_0$) and excess temperature ($\Delta T_0$) at the centre line of a fire plume in the source term flow regime have been presented in Eqs. (8b) and (8c). These values approach their ambient values, as the radial distance from the plume centre line increases. We present in the following a model for determining the equivalent mean velocity and excess temperature for uniform (i.e., top-hat) profiles of the plume cross-sections, under the condition that convective heat energy is conserved.

We assume Gaussian radial profiles of the excess temperature, $\Delta T(r)$, and the mean velocity, $u(r)$ (Heskestad, 2016),

$$\Delta T(r) = \Delta T_0 exp\left(-\left(\frac{r}{\sigma_{\Delta T}}\right)^2\right), \quad \text{(B1a)}$$

$$u(r) = u_0 exp\left(-\left(\frac{r}{\sigma_u}\right)^2\right), \quad \text{(B1b)}$$

where $r$ is the radial distance measured from the centre line of the plume; and $\sigma_{\Delta T}$ and $\sigma_u$ are the measures of the plume width corresponding to the radial distributions of excess temperature and velocity, respectively. The density of the plume is assumed to have a constant value within each cross-section of the plume, equal to the centre line value ($\rho_0$).

The radius of the plume, $r_{\Delta T}$, has been defined in terms of $\Delta T_0$ (Eq. (8a)). A velocity radius ($r_u$) can be defined correspondingly: let $r_u$ be the plume radius at the point, in which the gas velocity has declined to $0.5u_0$ (Heskestad, 2016). The temperature and velocity profiles have in general differing scales, i.e.,

$$r_u = a r_{\Delta T}. \quad \text{(B2)}$$

According to Heskestad (2016), an optimal value is $a$ = 1.1, based on the most reliable measurements (George Jr. et al., 1977).

https://doi.org/10.5194/gmd-2021-88
Preprint. Discussion started: 25 May 2021


Geoscientific Model Development Discussions

Applying Eqs. (B1a-b) and the definitions of the radiuses $r_{\Delta T}$ and $r_u$ yields an estimate for the measures of the plume widths,

$$\sigma_x = \left(ln(2)\right)^{-1/2} r_x \equiv b r_x, \tag{B3}$$

where the subscript $x$ is either $u$ or $\Delta T$; and $b \approx 1.201$.

The equivalent top-hat excess temperature ($\Delta T$) and velocity ($u$) of the plume can derived by integrating Eqs. (B1a) and (B1b), and using the relations (B3),

$$\Delta T = \Delta T_0 R^{-1} \int_0^R exp\left(-\left(\frac{r}{b r_{\Delta T}}\right)^2\right) dr, \tag{B4a}$$

$$u = u_0 R^{-1} \int_0^R exp\left(-\left(\frac{r}{b r_u}\right)^2\right) dr = u_0 R^{-1} \int_0^R exp\left(-\left(\frac{r}{ab r_{\Delta T}}\right)^2\right) dr, \tag{B4b}$$

where $R$ is a radial distance from the centre of the plume.

Equations (B4a-b) can be written more simply in terms of the error function (*erf*), defined as

$$\int_0^R exp\left(-\left(\frac{r}{\sigma}\right)^2\right) dr = \frac{\sqrt{\pi}}{2} \sigma \, erf\left(\frac{R}{\sigma}\right). \tag{B5}$$

Therefore

$$\Delta T = \Delta T_0 \frac{\sqrt{\pi}}{2} \frac{b r_{\Delta T}}{R} erf\left(\frac{R}{b r_{\Delta T}}\right) = \Delta T_0 \frac{\sqrt{\pi}}{2} \frac{b}{c} erf\left(\frac{c}{b}\right) \equiv \Delta T_0 s_{\Delta T}, \tag{B6a}$$

$$u = u_0 \frac{\sqrt{\pi}}{2} \frac{ab r_{\Delta T}}{R} erf\left(\frac{R}{ab r_{\Delta T}}\right) = u_0 \frac{\sqrt{\pi}}{2} \frac{ab}{c} erf\left(\frac{c}{ab}\right) \equiv u_0 s_u, \tag{B6b}$$

where $c = R/r_{\Delta T}$, and $s_{\Delta T}$ and $s_u$ are dimensionless scale factors.

https://doi.org/10.5194/gmd-2021-88
Preprint. Discussion started: 25 May 2021


Geoscientific Model Development Discussions

Substituting $\Delta T_0$ and $u_0$ in Eqs. (B1a-b) to Eqs. (B6a-b), and requiring conservation of convective heat flux yields

$$s_{\Delta T} s_u = \frac{\pi}{4}\frac{ab^2}{c^2} erf\left(\frac{c}{b}\right) erf\left(\frac{c}{ab}\right) = C^{-1}. \quad \text{(B7)}$$

Equation (B7) is an implicit function for $c$, which can be solved numerically. Let us next examine the properties of this numerical problem. From Eq. (B7) we may define a function $f$

$$f(x) = \frac{1}{x^2} erf(x) erf\left(\frac{x}{a}\right) - \frac{4}{\pi a C} \equiv \frac{1}{x^2} erf(x) erf\left(\frac{x}{a}\right) - D, \quad \text{(B8)}$$

where $x = c\,b\text{-}1 > 0$; and $D > 0$ is a constant. The function $f$ is continuous and differentiable. The zero point(s) of $f$ straightforwardly determine the radius $R$, and the scale factors $s_{\Delta T}$ and $s_u$.

Further, as $0 < erf(x) \leq 1$, for $x > 0$,

$$f(x) = \frac{1}{x^2} erf(x) erf\left(\frac{x}{a}\right) - D \leq \frac{1}{x^2} - D. \quad \text{(B9)}$$

Thus, $f(x) < 0$ for $x > D^{-1/2}$, and any possible zero points of $f$ are within $(0, D^{-1/2}]$. Applying the series expansion (e.g. Abramowitz and Stegun, 1972)

$$erf(x) = \frac{2}{\sqrt{\pi}} x\left(1 - \frac{x^2}{3} + \frac{x^4}{10} - \frac{x^6}{42} + \cdots\right), \quad \text{(B10)}$$

yields

$$\lim_{x \to 0} f(x) = \frac{4}{\pi a} - D = \frac{4}{\pi a}\left(1 - \frac{1}{C}\right). \quad \text{(B11)}$$

https://doi.org/10.5194/gmd-2021-88
Preprint. Discussion started: 25 May 2021




Hence, for

$$C > 1, \tag{B12}$$

$f$ is positive as $x \to 0$, and $f$ has at least one zero point. Function $f$, assuming typical values of experimental coefficients $a$, $C_1$, $C_2$ and $C_3$, has been illustrated in Fig. B1.

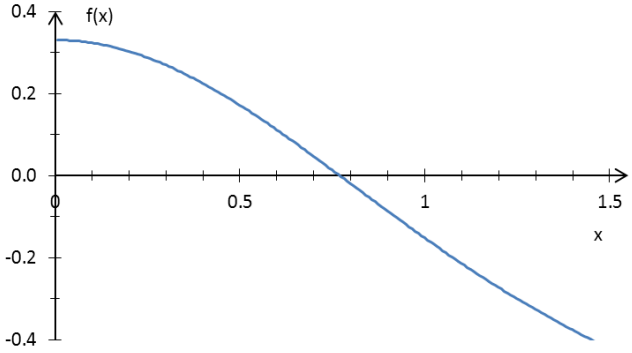


**Figure B1. Function $f(x)$ (defined in Eq. (B9)), with $a$ = 1.1, $C_1$ = 0.12, $C_2$ = 3.4 and $C_3$ = 9.1.**

For $C < 1$, the conservation of convective heat energy cannot be achieved applying the presented method. Therefore, any possible zero value of $f$ is physically irrelevant. The zero value of $f(x)$ was estimated numerically ($x \in (0, D^{-1/2}]$) with a combination of linear interpolation, inverse quadratic interpolation, and bisection (Brent, 1971). Assuming that $C_1$ = 0.12, $C_2$ = 3.4, $C_3$ = 9.1 and $a$ = 1.1, yields

$$c \approx 0.92578, \tag{B13a}$$
$$s_{\Delta T} \approx 0.83280, \tag{B13b}$$
$$s_u \approx 0.85788. \tag{B13c}$$

The value of $c$ (Eq. (B13a)) implies that the temperature and velocity profiles are integrated almost (93 %) up to the point where the temperature excess has been declined to $0.5\Delta T_0$, whereas the velocity profile is integrated up to 84 % of $r_u$. The top-hat excess temperature ($\Delta T$) and velocity ($u$) are 83 % and 86 % of their centre line values, respectively, as written in Eqs. (12a-b).

https://doi.org/10.5194/gmd-2021-88
Preprint. Discussion started: 25 May 2021




Clearly, $s_{\Delta T} = s_u$ for distributions of $\Delta T(r)$ and $u(r)$ with equal scales ($a = 1$). Further, for $a = 1$, $s_{\Delta T} = s_u = (\pi C_1^2 C_2 C_3)^{-1/2}$. For the same coefficients $C_i$ as above, yields $s_{\Delta T} = s_u \approx 0.84525$.

https://doi.org/10.5194/gmd-2021-88
Preprint. Discussion started: 25 May 2021


Geoscientific Model Development Discussions

## Appendix C. Detailed modelling of the selected application areas

Semi-empirical models of mass burning rate are presented in the following for liquid pool and forest fires. Mass fluxes of the emitted chemical compounds (e.g. CO, $CO_2$) from the fire are, by definition, determined employing the modelled mass burning rate and emission factors.

### C1. Mass fluxes of pollutants originated from liquid pool fires

Hottel (1959) suggested how to analyze liquid pool burning, according to heat transfer principles (Babrauskas, 1983). According to Hottel (1959), the mass burning rate is governed by the heat exchange between the flames and the pool surface. The heat exchange mechanisms are (a) radiant flux from the flames into the pool, (b) convective flux from the flames into the pool, (c) re-radiant heat loss ($Q_{rr}$) due to high temperature of the pool and (d) conduction losses and non-steady terms ($Q_{misc}$).

The term $Q_{rr}$ is commonly small, and quantitative expressions for $Q_{misc}$ are usually not available (Babrauskas, 1983). For simplicity, the terms $Q_{rr}$ and $Q_{misc}$ are therefore customarily ignored (Babrauskas, 1983). Hottel (1959) analyzed the experimental data of Blinov and Khudiakov (1957), concluding that two burning regimes are possible: radiatively dominated burning for larger pools and convectively dominated burning for smaller pools. The distinction between the two regimes can be drawn at the pool diameter of approximately 0.2 m (Hottel 1959; Babrauskas, 1983; Chatris et al., 2001). For the purposes of fire hazard analysis, liquid pool fires will rarely be significantly dangerous, if these are smaller than about 0.2 m in diameter (Babrauskas, 2016). It is therefore commonly necessary to treat only pool burning in the radiative regime.

Zabetakis and Burgess (1961) suggested (cf. Babrauskas, 1983; Chatris et al., 2001; Brambilla and Manca, 2009), based on the work of Hottel (1959), the following relationship to represent the mass burning rate ($q_{m,f}$) of a liquid pool in the radiative dominated regime:

$$q_{m,f} = q_{m,\infty} A\left(1 - e^{-k\beta d}\right), \tag{C1}$$

where $q_{m,\infty}$ is the mass burning rate per unit area of an infinite-diameter pool; $A$ is the surface area of the burning liquid pool; $k$ is the extinction coefficient of the flame; $\beta$ is a mean-beam-length corrector; and $d$ is the diameter of pool. For small $d$ the flames are said to be optically thin, while for larger $d$ the

https://doi.org/10.5194/gmd-2021-88
Preprint. Discussion started: 25 May 2021


Geoscientific Model Development Discussions

flames become optically thick (Babrauskas, 1983). For optically thick flames, a further increase in $d$ does not result into a corresponding increase in back radiation into the pool. Such attenuation is accounted for by the coefficient $k\beta$ (Brambilla and Manca, 2009).

Values of the empirical coefficients $q_{m,\infty}$ and $k\beta$ for a variety of fuels have been proposed by, for instance, Babrauskas (1983), Rew et al. (1997) and Chatris et al. (2001). The surface area of the burning liquid pool and the name of the liquid fuel have to be provided as input data for the model.

Experimental values of the lower heat of complete combustion ($H_c$) for various burning fuels (liquids) have been tabulated by, for example, Babrauskas (1983), McGrattan et al. (2000) and Hurley (2016).

The total heat generated by a liquid pool fire is here assumed to be propagated only through convective and radiative processes, i.e. $\varepsilon_o = 0 \Leftrightarrow \varepsilon_c = 1 - \varepsilon_r$. Radiometer measurements from large fire experiments involving different combustible liquids (such as crude oil, heptane and kerosene) suggest that the radiative fraction ($\varepsilon_r$) decreases with increasing fire diameter ($d$), according to (McGrattan et al., 2000)

$$\varepsilon_r = \varepsilon_{max} e^{-kd}, \tag{C2}$$

where $\varepsilon_{max} = 0.35$; and $k = 0.05$ m$^{-1}$.

Yield ($y_i$) of a fire product $i$ is defined as the ratio of mass generation rate of $i$ to mass burning rate of the combusting fuel (e.g. Tewarson, 1980; Khan et al., 2016)

$$y_i = \frac{m_{w,i} q_{n,i}}{q_{m,f}}, \tag{C3}$$

where $m_{w,i}$ is the molecular weight of species $i$; and $q_{n,i}$ is the molar flux of species $i$. Experimental values of yields under well-ventilated fire conditions have been listed by, for instance, Ross et al. (1996) and Hurley (2016).

https://doi.org/10.5194/gmd-2021-88
Preprint. Discussion started: 25 May 2021


Geoscientific Model Development Discussions

Molar fluxes ($q_n$,$i$) of gaseous fire products are calculated using Eq. (C3). Finally, molar flux of air can be calculated utilizing Eqs. (10) and (11).

Examples of fuel property data are shown in Table C1.

Table C1. Examples of the fuel property data (Babrauskas, 1983, Hurley, 2016). The quantities $H_c$, $q_{m,\infty}$ and $k\beta$ are defined in the text, and $y_{CO2}$, $y_{CO}$, $y_{hc}$ and $y_s$ are the yields of $CO_2$, CO, hydrocarbons and soot, respectively. Dashes indicate that either there are no measurements or their values are less than 0.001.

| Material | $H_c$ | $q_{m,\infty}$ | $k\beta$ | $y_{CO2}$ | $y_{CO}$ | $y_{hc}$ | $y_s$ |
|---|---|---|---|---|---|---|---|
| | kJ kg$^{-1}$ | kg (m$^2$ s)$^{-1}$ | m$^{-1}$ | g g$^{-1}$ | g g$^{-1}$ | g g$^{-1}$ | g g$^{-1}$ |
| Acetone ($C_3H_6O$) | 25800 | 0.041 | 1.9 | 2.14 | 0.003 | 0.001 | 0.014 |
| Benzene ($C_6H_6$) | 40100 | 0.085 | 2.7 | 2.33 | 0.067 | 0.018 | 0.181 |
| Butane ($C_4H_{10}$) | 45700 | 0.078 | 2.7 | 2.85 | 0.007 | 0.003 | 0.029 |
| Heptane ($C_7H_{16}$) | 44600 | 0.101 | 1.1 | 2.85 | 0.01 | 0.004 | 0.037 |
| Kerosene | 43200 | 0.039 | 3.5 | 2.83 | 0.012 | 0.004 | 0.042 |
| LNG (mostly $CH_4$) | 50000 | 0.078 | 1.1 | 2.72 | – | – | – |
| LPG (mostly $C_3H_8$) | 46000 | 0.099 | 1.4 | 2.85 | 0.005 | 0.001 | 0.024 |

**C2. Mass fluxes of pollutants originated from forest fires**

McAllister and Finney (2016a and 2016b) have evaluated the mass burning rate of wildland fires. Wood cribs, such as the one presented in Fig. (C1), have been used in fire testing. Block (1971) developed a theoretical model of the crib burning rate. Heskestad (1973) combined the experimental results of Gross (1962) and Block (1971) with the theoretical findings of Block (1971). This resulted in a relation of the mass burning rate ($q_{m,f}$) on the porosity ($\phi$) of the crib (see also McAllister and Finney, 2016a),

$$\frac{10^3 q_{m,f}}{A_s b^{-1/2}} = f(\phi), \qquad \text{(C4)}$$

https://doi.org/10.5194/gmd-2021-88
Preprint. Discussion started: 25 May 2021


Geoscientific Model Development Discussions

where $A_s$ is the exposed surface area of the sticks in the crib; and $b$ is the thickness of the sticks (defined in Fig. C1). The functional form of $f$ was found to be approximately (McAllister and Finney, 2016a)

$$f(\phi) = 1 - e^{-50\phi}. \quad \text{(C5)}$$

For well-ventilated cribs or loosely-packed porous burning cribs, $\phi$ is large and $f(\phi)$ approaches unity.

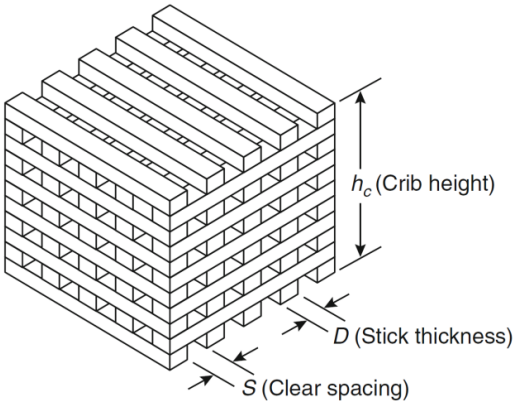


**Figure C1. General arrangement of a wood crib (Babrauskas, 2016).**

Wildland fuel beds are commonly porous, i.e., the porocity is large (McAllister and Finney, 2016a). However, according to Tang (2017), both well-ventilated and under-ventilated fires can exist in forested regions. We have assumed in this study, for simplicity, that the fuel beds are porous ($f(\phi) = 1$).

Let us define the diameter of a tree trunk at human breast height, $d_{bh}$. Commonly $d_{bh}$ is measured approximately at a height of 1.3 m. Assuming that $d_{bh}$ is a representative value of $b$, we can approximate the mass burning rate of a porous wildland fire to be

$$q_{m,f} \approx 10^{-3} A_s d_{bh}^{-1/2}. \quad \text{(C6)}$$

Assuming that all of the trees from the ground to treetop are on fire, the exposed surface area of one tree is equal to $\pi d_{bh} h_t$, where $h_t$ is the average height of the burning trees. The exposed area of all the trees can therefore be approximated by

https://doi.org/10.5194/gmd-2021-88
Preprint. Discussion started: 25 May 2021


Geoscientific Model Development Discussions

$$A_s = \pi d_{bh} h_t n_t A, \quad \text{(C7)}$$

where $n_t$ is the number of burning trunks per unit forest area burning; and $A$ is the area of forest on fire.

Heat generated by a forest fire is estimated from Eqs. (1) and (C6). The lower heat of combustion ($H_c$) of woody fuel ranges typically from 17.8 to 20.4 MJ kg$^{-1}$ (e.g. Trentmann et al. 2006; Hurley, 2016). We have therefore applied the middle value within this range ($H_c$ = 19.1 MJ kg$^{-1}$).

The fraction of total energy released by combustion that is available for convection depends on the ambient and fuel conditions (Trentmann et al., 2006; Freitas et al., 2010; Kukkonen et al., 2014). Laboratory experiments of biomass burning (Freeborn et al., 2008) have indicated a mean convective fraction of 51.8 ± 9.0 % (determined in terms of higher heat of combustion, i.e., including latent heat released during condensation of water vapour generated by the fire). We have assumed that 55 % of the total heat generated by a forest fire is available for convection ($\varepsilon_c$ = 0.55). This is simply in the middle of the commonly accepted range from 0.4 to 0.8 (Trentmann et al., 2002; Freitas et al., 2010).

The emission factor can be defined to be the amount of the chemical species released per mass of dry biomass burned (e.g., Andreae and Merlet, 2001). Therefore, emission factor is equal to the yield of combustion products ($y_i$). Data on emission factors for various types of biomass burning have been presented by, for instance, Lemieux et al. (2004), Akagi et al. (2011), Kaiser et al. (2012) and Urbanski (2014a). The current model version applies the emission factors, which are applicable for land cover class of extratropical forest, presented by Kaiser et al. (2012). The extratropical forest class includes forest types typically found in the northern hemisphere (Kaiser et al., 2012).

For simplicity, particles formed in a forest or a liquid pool fire are assumed to be spherical. Further, they are assumed to be 2.5 μm in aerodynamical diameter having the density of water, i.e. the unit density = 1 kg dm$^{-3}$.

https://doi.org/10.5194/gmd-2021-88
Preprint. Discussion started: 25 May 2021


Geoscientific Model Development Discussions

**Appendix D. The extraction and pre-processing of meteorological data.**

The program can use either real-time or forecasted meteorological data produced by the numerical weather prediction (NWP) model HARMONIE. HARMONIE is a state-of-the-art NWP model, which has been widely used and developed in Europe. The main limitation of the HARMONIE model, as applied in the present study, is its fairly limited geographic domain.

HARMONIE is a non-hydrostatic convection-permitting NWP model. The horizontal grid spacing of the model is 0.022° (approximately 2.5 km). The vertical grid consists of 65 vertical hybrid levels. In this study, we applied the HARMONIE version cy40h11, which is in operational use at the FMI. Meteorological forecasts are continuously produced four times a day, with a temporal resolution of one hour and a forecast length of about two days ahead in time.

Most of the meteorological variables required by the BUOYANT model are directly available from HARMONIE forecasts. The vertical structure of the atmosphere in the BUOYANT model assumed to comprise three distinct layers: the atmospheric boundary layer (ABL), capping inversion layer and upper layer (Kukkonen et al., 2014). Variables that are readily available in HARMONIE include height of the ABL and the vertical profiles of the temperature, pressure and wind speed.

In the ABL the vertical variations of wind speed and temperature are in this study assumed to be described with profiles based on the Monin-Obukhov similarity theory, as presented by Kukkonen et al. (2014). Monin-Obukhov length is estimated based on the values of the turbulent momentum stress near the ground surface, as forecasted by HARMONIE. The two-layered thermal structure above ABL (inversion and upper layers) is evaluated by applying the HARMONIE predictions with a method modified from Fochesatto (2015).

In the upper layer (above the inversion layer), the wind speed is assumed to be constant (representing the geostrophic flow), whereas within the inversion layer the wind speed is assumed to change with constant gradient from its value at the top of the ABL to the geostrophic value. The constant geostrophic wind speed was assumed to be equal to the arithmetic mean of HARMONIE forecasts between the top of the inversion layer and the height of 5 km.

https://doi.org/10.5194/gmd-2021-88
Preprint. Discussion started: 25 May 2021


Geoscientific Model Development Discussions

## Code and data availability

The code and the relevant data are available in Zenodo at https://doi.org/10.5281/zenodo.4744300 (Kukkonen et al., 2021). These contain the source code of the BUOYANT model (v4.20), the technical reference of the model, the user manual of the model and the model input data corresponding to the work described in this paper. The model code, documentation and the input data are published under the license of Creative Commons Attribution 4.0 International.

The experimental data of the RxCADRE campaign used in this paper can be downloaded from the Research Data Archive of the U.S. Department of Agriculture (Hudak et al., 2016a; Jimenez and Butler, 2016; Seto and Clements, 2015a and 2015b; Urbanski, 2014b).

## Author contribution

The research version of the BUOYANT model, including the source term module, has been developed by Juha Nikmo, Jaakko Kukkonen and Kari Riikonen. All the authors have contributed to the development of the operational model version. Ilmo Westerholm, Pekko Ilvessalo, Tuomo Bergman and Klaus Haikarainen performed most of the research and coding that was necessary for the functioning of the operational model. Juha Nikmo performed the model computations for the evaluation of the model. Jaakko Kukkonen was the leader and coordinator of the project, in which this work was performed. Jaakko Kukkonen and Juha Nikmo prepared the manuscript, with contributions from all co-authors.

## Conflicting interests

The authors declare that they have no conflict of interest.

## Acknowledgements

We would like to thank for the financial support of the project “The assessment of the dispersion of pollutants from fires, for the needs of rescue services”, funded by the Fire Protection Fund in Finland. Ministry of the Interior in Finland, especially Director General for Rescue Services Dr. Janne Koivukoski, is thanked for the continuous support of the project. We also wish to thank the following persons at the

https://doi.org/10.5194/gmd-2021-88
Preprint. Discussion started: 25 May 2021


FMI for their contributions and comments in developing the operational model version: Mr. Juha Jääskeläinen, Mr. Ari-Juhani Punkka, Dr. Ari Karppinen, Dr. Antti Hellsten and Prof. Mikhail Sofiev. The authors also thank D.Sc. Matti Katila and his co-workers at Natural Resources Institute Finland for valuable advices regarding the use of the Multi-Source National Forest Inventory of Finland.

**References**

Abramowitz, M., and Stegun, I.A. (eds.): Handbook of mathematical functions with formulas, graphs, and mathematical tables, Tenth printing, National Bureau of Standards, United States Department of Commerce, 1046 pp., 1972.

Achtemeier, G.L., Goodrick, S.A., and Liu, Y.: Modeling multiple-core updraft plume rise for an aerial ignition prescribed burn by coupling Daysmoke with a cellular automata fire model, Atmosphere, 3, 352-376, doi:https://doi.org/10.3390/atmos3030352, 2012.

Akagi, S.K., Yokelson, R.J., Wiedinmyer, C., Alvarado, M.J., Reid, J.S., Karl, T., Crounse, J.D., and Wennberg, P.O.: Emission factors for open and domestic biomass burning for use in atmospheric models, Atmos. Chem. Phys., 11, 4039-4072, doi:https://doi.org/10.5194/acp-11-4039-2011, 2011.

Anderson, G.K., Sandberg, D.V., and Norheim, R.A.: Fire Emission Production Simulator (FEPS) User's Guide, Version 1.0, https://www.fs.fed.us/pnw/fera/feps/FEPS_users_guide.pdf, last access 21 September 2020, 2004.

Andreae, M.O., and Merlet, P.: Emission of trace gases and aerosols from biomass burning, Global Biochem. Cy., 15, 955-966, doi:https://doi.org/10.1029/2000GB001382, 2001.

Babrauskas, V.: Estimating large pool fire burning rates, Fire Technol., 19, 251-261, doi:https://doi.org/10.1007/BF02380810, 1983.

Babrauskas, V.: Heat release rates, in: SFPE Handbook of Fire Protection Engineering, edited by Hurley, M.J., Fifth edition, ISBN 978-1-4939-2564-3, Springer Science+Business Media LLC New York, 799-904, doi:https://doi.org/10.1007/978-1-4939-2565-0_26, 2016.

https://doi.org/10.5194/gmd-2021-88
Preprint. Discussion started: 25 May 2021


Geoscientific Model Development Discussions

Beyler, C.L.: Fire hazard calculations for large, open hydrocarbon fires, in: SFPE Handbook of Fire Protection Engineering, edited by Hurley, M.J., Fifth edition, ISBN 978-1-4939-2564-3, Springer Science+Business Media LLC New York, 2591-2663, doi:https://doi.org/10.1007/978-1-4939-2565-0_66, 2016.

Blinov, V.I., and Khudiakov, G.N.: Certain laws governing diffusive burning of liquids. Dokl Akad Nauk SSSR+ 113, 1094-1098, 1957.

Block, J.A.: A theoretical and experimental study of nonpropagating free-burning fires, Symposium (International) on Combustion, 13, 971-978, doi:https://doi.org/10.1016/S0082-0784(71)80097-8, 1971.

Brambilla, S., and Manca, D.: Accidents involving liquids: A step ahead in modeling pool spreading, evaporation and burning, J. Hazard. Mater., 161, 1265-1280, doi:https://doi.org/10.1016/j.jhazmat.2008.04.109, 2009.

Brent, R.P.: An algorithm with guaranteed convergence for finding a zero of a function, Comput. J., 14, 422-425, doi:https://doi.org/10.1093/comjnl/14.4.422, 1971.

Chatris, J.M., Quintela, J., Folch, J., Planas, E., Arnaldos, J., and Casal, J.: Experimental study of burning rate in hydrocarbon pool fires. Combust. Flame, 126, 1373-1383, doi:https://doi.org/10.1016/S0010-2180(01)00262-0, 2001.

Clements, C.B., Kochanski, A.K., Seto, D., Davis, B., Camacho, C., Lareau, N.P., Contezac, J., Restaino, J., Heilman, W.E., Krueger, S.K., Butler, B., Ottmar, R.D., Vihnanek, R., Flynn, J., Filippi, J.-B., Barboni, T., Hall, D.E., Mandel, J., Jenkins, M.A., O'Brien, J., Hornsby, B., and Teske, C.: The FireFlux II experiment: a model-guided field experiment to improve understanding of fire–atmosphere interactions and fire spread, Int. J. Wildland Fire, 28, 308-326, doi:https://doi.org/10.1071/WF18089, 2019.

https://doi.org/10.5194/gmd-2021-88
Preprint. Discussion started: 25 May 2021


Clements, C.B., Lareau, N.P., Seto, D., Contezac, J., Davis, B., Teske, C., Zajkowski, T.J., Hudak, A.T., Bright, B.C., Dickinson, M.B., Butler, B.W., Jimenez, D., and Hiers, J.K.: Fire weather conditions and fire-atmosphere interactions observed during low-intensity prescribed fires - RxCADRE 2012, Int. J. Wildland Fire, 25, 90-101, doi:https://doi.org/10.1071/WF14173, 2016.

de Groot, W.J., Landry, R., Kurz, W.A., Anderson, K.R., Englefield, P., Fraser, R.H., Hall, R.J., Banfield, E., Raymond, D.A., Decker, V., Lynham, T.J., and Pritchard, J.M.: Estimating direct carbon emissions from Canadian wildland fires, Int. J. Wildland Fire, 16, 593-606, doi:https://doi.org/10.1071/WF06150, 2007.

de Groot, W.J., Pritchard, J.M., and Lynham, T.J.: Forest floor fuel consumption and carbon emissions in Canadian boreal forest fires, Can. J. Forest Res., 39, 367-382, doi:https://doi.org/10.1139/X08-192, 2009.

Dennis, A., Fraser, M., Anderson, S., and Allen, D.: Air pollutant emissions associated with forest, grassland, and agricultural burning in Texas, Atmos. Environ., 36, 3779-3792, doi:https://doi.org/10.1016/S1352-2310(02)00219-4, 2002.

Devenish, B.J., Rooney, G.G.,Webster, H.N., and Thomson, D.J.: The entrainment rate for buoyant plumes in a crossflow, Bound.-Lay. Meteorol., 134, 411-439, doi:https://doi.org/10.1007/s10546-009-9464-5, 2010.

Dickinson, M.B., Hudak, A.T., Zajkowski, T., Loudermilk, E.L., Schroeder, W., Ellison, L., Kremens, R.L., Holley, W., Martinez, O., Paxton, A., Bright, B.C., O'Brien, J.J., Hornsby, B., Ichoku, C., Faulring, J., Gerace, A., Peterson, D., and Mauceri, J.: Measuring radiant emissions from entire prescribed fires with ground, airborne and satellite sensors - RxCADRE 2012, Int. J. Wildland Fire, 25, 48-61, doi:https://doi.org/10.1071/WF15090, 2016.

Drysdale, D.D.: Ignition of liquids, in: SFPE Handbook of Fire Protection Engineering, edited by Hurley, M.J., Fifth edition, ISBN 978-1-4939-2564-3, Springer Science+Business Media LLC New York, 554-580, doi:https://doi.org/10.1007/978-1-4939-2565-0_18, 2016.


Dupuy, J.L., Maréchal, J., and Morvan, D.: Fires from a cylindrical forest fuel burner: combustion dynamics and flame properties, Combust. Flame, 135, 65-76, doi:https://doi.org/10.1016/S0010-2180(03)00147-0, 2003.

Fay, J.A.: Model of large pool fires, J. Hazard. Mater., 136, 219-232, doi:https://doi.org/10.1016/j.jhazmat.2005.11.095, 2006.

Fingas, M.: Review of emissions from oil fires, in: Proceedings of 2014 International Oil Spill Conference, 1795-1805, doi:https://doi.org/10.7901/2169-3358-2014.1.1795, 2014.

Fochesatto, G.J.: Methodology for determining multilayered temperature inversions, Atmos. Meas. Tech., 8, 2051-2060, doi:https://doi.org/10.5194/amt-8-2051-2015, 2015.

Freeborn, P.H., Wooster, M.J., Hao, W.M., Ryan, C.A., Nordgren, B.L., Baker, S.P., and Ichoku, C.: Relationships between energy release, fuel mass loss, and trace gas and aerosol emissions during laboratory biomass fires, J. Geophys. Res., 113, D01301, doi:https://doi.org/10.1029/2007JD008679, 2008.

Freitas, S.R., Longo, K.M., Chatfield, R., Latham, D., Dias, M.A.F.S., Andreae, M.O., Prins, E., Santos, J.C., Gielow, R., and Carvalho Jr., J.A.: Including the sub-grid scale plume rise of vegetation fires in low resolution atmospheric transport models, Atmos. Chem. Phys., 7, 3385-3398, doi:https://doi.org/10.5194/acp-7-3385-2007, 2007.

Freitas, S.R., Longo, K.M., Trentmann, J., and Latham, D.: Technical Note: Sensitivity of 1-D smoke plume rise models to the inclusion of environmental wind drag, Atmos. Chem. Phys., 10, 585-594, doi:https://doi.org/10.5194/acp-10-585-2010, 2010.

Gassó, S., and Hegg, D.A.: Comparison of columnar aerosol optical properties measured by the MODIS airborne simulator with in situ measurements: A case study, Remote Sens. Environ., 66, 138-152, doi:https://doi.org/10.1016/S0034-4257(98)00052-2, 1998.

https://doi.org/10.5194/gmd-2021-88
Preprint. Discussion started: 25 May 2021


George Jr., W.K., Alpert, R.L., and Tamanini, F.: Turbulence measurements in an axisymmetric buoyant plume, Int. J. Heat Mass Tran., 20, 1145-1154, doi:https://doi.org/10.1016/0017-9310(77)90123-5, 1977.

Gross, D. Experiments on the burning of cross piles of wood, J. Res. NBS C Eng. Inst., 66C, 99-105, doi:https://doi.org/10.6028/jres.066C.010, 1962.

Grove, B.S., and Quintiere, J.G.: Calculating entrainment and flame height in fire plumes of axisymmetric and infinite line geometries, J. Fire Prot. Eng., 12, 117-137, doi:https://doi.org/10.1177/10423910260620464, 2002.

Hertzberg, M.: The theory of free ambient fires. The convectively mixed combustion of fuel reservoirs, Combust. Flame, 21, 195-209, doi:https://doi.org/10.1016/S0010-2180(73)80024-0, 1973.

Heskestad, G.: Modeling of enclosure fires, Symposium (International) on Combustion, 14, 1021-1030, doi:https://doi.org/10.1016/S0082-0784(73)80092-X, 1973.

Heskestad, G.: Engineering relations for fire plumes, Fire Safety J., 7, 25-32, doi:https://doi.org/10.1016/0379-7112(84)90005-5, 1984.

Heskestad, G.: Dynamics of the fire plume, Philos. T. Roy. Soc. A, 356, 2815-2833, doi:https://doi.org/10.1098/rsta.1998.0299, 1998.

Heskestad, G.: Fire plumes, flame height, and air entrainment, in: SFPE Handbook of Fire Protection Engineering, edited by: Hurley, M.J., Fifth edition, ISBN 978-1-4939-2564-3, Springer Science+Business Media LLC New York, 396-428, doi:https://doi.org/10.1007/978-1-4939-2565-0_13, 2016.

Hobbs, P.V., Reid, J.S., Herring, J.A., Nance, J.D., Weiss, R.E., Ross, J.L., Hegg, D.A., Ottmar, R.D., and Liousse, C.: Particle and trace-gas measurements in the smoke from prescribed burns of forest


products in the Pacific Northwest, in: Biomass Burning and Global Change, edited by: Levine, J.S., MIT Press, Cambridge, MA, 697–715, 1996.

Hoelzemann, J.J., Schultz, M.G., Brasseur, G.P., and Granier, C.: Global Wildland Fire Emission Model (GWEM): Evaluating the use of global area burnt satellite data, J. Geophys. Res., 109, D14S04, doi:https://doi.org/10.1029/2003JD003666, 2004.

Hostikka, S., McGrattan, K.B., and Hamins, A.: Numerical modeling of pool fires using LES and Finite Volume Method for radiation, Fire Safety Science, 7, 383-394, doi:https://doi.org/10.3801/IAFSS.FSS.7-383, 2003.

Hottel, H.C.: Certain laws governing diffusive burning of liquids by V. I. Blinov and G. N. Khudiakov, Fire Research Abstracts and Reviews 1, 41-44, 1959.

Hudak, A.T., Bright, B.C., Kremens, R.L., and Dickinson, M.B.: RxCADRE 2011 and 2012: Wildfire Airborne Sensor Program long wave infrared calibrated image mosaics, Fort Collins, CO, Forest Service Research Data Archive, doi:https://doi.org/10.2737/RDS-2016-0008, 2016a.

Hudak, A.T., Dickinson, M.B., Bright, B.C., Kremens, R.L., Loudermilk, E.L., O'Brien, J.J., Hornsby, B.S., and Ottmar, R.D.: Measurements relating fire radiative energy density and surface fuel consumption - RxCADRE 2011 and 2012, Int. J. Wildland Fire, 25, 25-37, doi:https://doi.org/10.1071/WF14159, 2016b.

Hurley, M.J. (ed.): SFPE Handbook of Fire Protection Engineering, Fifth edition, ISBN 978-1-4939-2564-3, Springer Science+Business Media LLC New York, 3493 pp., doi:https://doi.org/10.1007/978-1-4939-2565-0, 2016.

Ichoku, C., Kahn, R., and Chin, M.: Satellite contributions to the quantitative characterization of biomass burning for climate modeling, Atmos. Res., 111, 1-28, doi:https://doi.org/10.1016/j.atmosres.2012.03.007, 2012.

https://doi.org/10.5194/gmd-2021-88
Preprint. Discussion started: 25 May 2021


1205 Ichoku, C., and Kaufman, Y.J.: A method to derive smoke emission rates from MODIS fire radiative energy measurements, IEEE T. Geosci. Remote, 43, 2636-2649, doi:https://doi.org/10.1109/TGRS.2005.857328, 2005.

ISO/IEC: Information technology -- Programming languages -- Fortran -- Part 1: Base language,
1210 ISO/IEC 1539-1:2004, 2004.

Ito, A., and Penner, J.E.: Global estimates of biomass burning emissions based on satellite imagery for the year 2000, J. Geophys. Res., 109, D14S05, doi:https://doi.org/10.1029/2003JD004423, 2004.

1215 Jimenez, D.M., and Butler, B.W.: RxCADRE 2012: RxCADRE 2012: In-situ fire behavior measurements, Fort Collins, CO, Forest Service Research Data Archive, doi:https://doi.org/10.2737/RDS-2016-0038, 2016.

Jirka, G.H.: Integral model for turbulent buoyant jets in unbounded stratified flows, Part I: Single round
1220 jet, Environ. Fluid Mech., 4, 1-56, doi:https://doi.org/10.1023/A:1025583110842, 2004.

Kahn, R.A., Chen, Y., Nelson, D.L., Leung, F.-Y., Li, Q., Diner, D.J., and Logan, J.A.: Wildfire smoke injection heights: Two perspectives from space, Geophys. Res. Lett., 35, 4-7, doi:https://doi.org/10.1029/2007GL032165, 2008.

1225

Kaiser, J.W., Heil, A., Andreae, M.O., Benedetti, A., Chubarova, N., Jones, L., Morcrette, J.-J., Razinger, M., Schultz, M.G., Suttie, M., and van der Werf, G.R.: Biomass burning emissions estimated with a global fire assimilation system based on observed fire radiative power, Biogeosciences, 9, 527-554, doi:https://doi.org/10.5194/bg-9-527-2012, 2012.

1230

Kaufman, Y.J., Remer, L.A., Ottmar, R.D., Ward, D.E., Li, R.-R., Kleidman, R., Fraser, R.S., Flynn, L., McDougal, D., and Shelton, G.: Relationship between remotely sensed fire intensity and rate of emission of smoke: SCAR-C experiment, in: Biomass Burning and Global Change, edited by: Levine, J.S., MIT Press, Cambridge, MA, 685–696, 1996.

1235

https://doi.org/10.5194/gmd-2021-88
Preprint. Discussion started: 25 May 2021


Khan, M.M., Tewarson, A., and Chaos, M.: Combustion characteristics of materials and generation of fire products, in: SFPE Handbook of Fire Protection Engineering, edited by Hurley, M.J., Fifth edition, ISBN 978-1-4939-2564-3, Springer Science+Business Media LLC New York, 1143-1232, doi:https://doi.org/10.1007/978-1-4939-2565-0_36, 2016.

Koseki, H.: Combustion properties of large liquid pool fires. Fire Technol., 25, 241-255, doi:https://doi.org/10.1007/BF01039781, 1989.

Kukkonen, J., Nikmo, J., Ramsdale, S.A., Martin, D., Webber, D.M., Schatzmann, M., and Liedtke, J.: Dispersion from strongly buoyant sources, in: Air Pollution Modeling and its Application XIII, edited by: Gryning, S.-E., and Batchvarova, E., Kluwer Academic/ Plenum Publishers, 539–547, 2000.

Kukkonen, J., Nikmo, J., Sofiev, M., Riikonen, K., Petäjä, T., Virkkula, A., Levula, J., Schobesberger, S., and Webber, D.M.: Applicability of an integrated plume rise model for the dispersion from wild-land fires, Geosci. Model Dev., 7, 2663-2681, doi:https://doi.org/10.5194/gmd-7-2663-2014, 2014.

Kukkonen, J., Nikmo, J., and Riikonen, K.: An emergency response model for evaluating the formation and dispersion of plumes originating from major fires (BUOYANT v4.20), https://doi.org/10.5281/zenodo.4744300, 2021.

Kung, H.-C., and Stavrianidis, P.: Buoyant plumes of large-scale pool fires, Symposium (International) on Combustion, 19, 905-912, doi:https://doi.org/10.1016/S0082-0784(82)80266-X, 1982.

Kung, H.-C., You, H.-Z., and Spaulding, R.D.: Ceiling flows of growing rack storage fires, Symposium (International) on Combustion, 21, 121-128, doi:https://doi.org/10.1016/S0082-0784(88)80238-8, 1988.

Lavoué, D., Liousse, C., Cachier, H., Stocks, B.J., and Goldammer, J.G.: Modeling of carbonaceous particles emitted by boreal and temperate wildfires at northern latitudes, J. Geophys. Res., 105, 26871-26890, doi:https://doi.org/10.1029/2000JD900180, 2000.

https://doi.org/10.5194/gmd-2021-88
Preprint. Discussion started: 25 May 2021


Lemieux, P.M., Lutes, C.C., and Santoianni, D.A.: Emissions of organic air toxics from open burning: a comprehensive review, Prog. Energ. Combust., 30, 1-32, doi:https://doi.org/10.1016/j.pecs.2003.08.001, 2004.

Liousse, C., Penner, J.E., Chuang, C., Walton, J.J., Eddleman, H., and Cachier, H.: A global three-dimensional model study of carbonaceous aerosols, J. Geophys. Res., 101, 19411–19432, doi:https://doi.org/10.1029/95JD03426, 1996.

Luketa, A., and Blanchat, T.: The phoenix series large-scale methane gas burner experiments and liquid methane pool fires experiments on water, Combust. Flame, 162, 4497-4513, doi:https://doi.org/10.1016/j.combustflame.2015.08.025, 2015.

Luketa-Hanlin, A.: A review of large-scale LNG spills: Experiments and modeling, J. Hazard. Mater. A132, 119-140, doi:https://doi.org/10.1016/j.jhazmat.2005.10.008, 2006.

Mallia, D.V., Kochanski, A.K., Urbanski, S.P., and Lin, J.C.: Optimizing smoke and plume rise modeling approaches at local scales, Atmosphere, 9, 166, doi:https://doi.org/10.3390/atmos9050166, 2018.

Mallia, D.V., Kochanski, A.K., Urbanski, S.P., Mandel, J., Farguell, A., and Krueger, S.K.: Incorporating a canopy parameterization within a coupled fire-atmosphere model to improve a smoke simulation for a prescribed burn, Atmosphere, 11, doi:https://doi.org/10.3390/atmos11080832, 2020.

Martin, D., Webber, D.M., Jones, S.J., Underwood, B.Y., Tickle, G.A., and Ramsdale, S.A.: Near- and intermediate-field dispersion from strongly buoyant sources, AEA Technology Report AEAT/1388, Warrington, 277 pp., 1997.

McAllister, S., and Finney, M.: The effect of wind on burning rate of wood cribs. Fire Technology, 52, 1035-1050, doi:https://doi.org/10.1007/s10694-015-0536-4, 2016a.

McAllister, S., and Finney, M.: Burning rates of wood cribs with implications for wildland fires. Fire Technology, 52, 1755-1777, doi:https://doi.org/10.1007/s10694-015-0543-5, 2016b.

https://doi.org/10.5194/gmd-2021-88
Preprint. Discussion started: 25 May 2021




McGrattan, K.B., Baum, H.R., and Hamins, A.: Thermal radiation from large pool fires, Report NISTIR 6546, National Institute of Standards and Technology, U.S. Department of Commerce, 31 pp., 2000.

Moisseeva, N., and Stull, R.: Capturing plume rise and dispersion with a coupled Large-Eddy Simulation: case study of a prescribed burn, Atmosphere, 10, 579, doi:https://doi.org/10.3390/atmos10100579, 2019.

Morton, B.R.: Modeling fire plumes, Symposium (International) on Combustion, 10, 973-982, doi:https://doi.org/10.1016/S0082-0784(65)80240-5, 1965.

Morton, B.R., Taylor, G., and Turner, J.S. Turbulent gravitational convection from maintained and instantaneous sources, P. Roy. Soc. A - Math. Phy., 234, 1-23, doi:https://doi.org/10.1098/rspa.1956.0011, 1956.

Mudan, K.S.: Thermal radiation hazards from hydrocarbon pool fires, Prog. Energ. Combust., 10, 59-80, doi:https://doi.org/10.1016/0360-1285(84)90119-9, 1984.

Mäkisara, K., Katila, M., and Peräsaari, J.: The Multi-Source National Forest Inventory of Finland - methods and results 2015, Natural resources and bioeconomy studies 8/2019, Natural Resources Institute Finland, Helsinki, 57 pp., http://urn.fi/URN:ISBN:978-952-326-711-4, 2019.

National Land Survey of Finland: Paikkatietoikkuna (Finnish National Geoportal), https://kartta.paikkatietoikkuna.fi/?lang=en, last access 5 February 2021, 2021.

Nielsen, K.P., Gleeson, E., and Rontu, L.: Radiation sensitivity tests of the HARMONIE 37h1 NWP model, Geosci. Model Dev., 7, 1433-1449, http://doi.org/10.5194/gmd-7-1433-2014, 2014.

Nieuwstadt, F.: The computation of the friction velocity $u_*$ and the temperature scale $T_*$ from temperature and wind velocity profiles by least-squares methods, Bound.-Lay. Meteorol., 14, 235-246, doi:https://doi.org/10.1007/BF00122621, 1978.

https://doi.org/10.5194/gmd-2021-88
Preprint. Discussion started: 25 May 2021


Nikmo, J., Tuovinen, J.-P., Kukkonen, J., and Valkama, I.: A hybrid plume model for local-scale dispersion, Publications on Air Quality 27, Finnish Meteorological Institute, Helsinki, 65 pp., 1997.

Nikmo, J., Tuovinen, J.-P., Kukkonen, J., and Valkama, I.: A hybrid plume model for local-scale atmospheric dispersion, Atmos. Environ., 33, 4389-4399, doi:https://doi.org/10.1016/S1352-2310(99)00223-X, 1999.

Olesen, H.R.: Datasets and protocol for model validation, Int. J. Environ. Pollut., 5, doi:https://doi.org/10.1504/IJEP.1995.028416, 693-701, 1995.

Ottmar, R.D.: Wildland fire emissions, carbon, and climate: Modeling fuel consumption, Forest Ecol. Manag., 317, 41-50, doi:https://doi.org/10.1016/j.foreco.2013.06.010, 2014.

Ottmar, R.D., Hiers, J.K., Butler, B.W., Clements, C.B., Dickinson, M.B., Hudak, A.T., O'Brien, J.J., Potter, B.E., Rowell, E.M., Strand, T.M., and Zajkowski, T.J.: Measurements, datasets and preliminary results from the RxCADRE project - 2008, 2011 and 2012, Int. J. Wildland Fire, 25, 1-9, doi:https://doi.org/10.1071/WF14161, 2016a.

Ottmar, R.D., Hudak, A.T., Prichard, S.J., Wright, C.S. Restaino, J.C., Kennedy, M.C., and Vihnanek, R.E.: Pre-fire and post-fire surface fuel and cover measurements collected in the southeastern United States for model evaluation and development - RxCADRE 2008, 2011 and 2012, Int. J. Wildland Fire, 25, 10-24, doi:https://doi.org/10.1071/WF15092, 2016b.

Peterson, D.L., and Hardy, C.C.: The RxCADRE study: a new approach to interdisciplinary fire research, Int. J. Wildland Fire, 25, doi:https://doi.org/10.1071/WFv25n1_FO, 2016.

Prichard, S., Larkin, N.S., Ottmar, R., French, N.H.F., Baker, K., Brown, T., Clements, C., Dickinson, M., Hudak, A., Kochanski, A., Linn, R., Liu, Y., Potter, B., Mell, W., Tanzer, D., Urbanski, S., and Watts, A.: The Fire and Smoke Model Evaluation Experiment - A plan for integrated, large fire-atmosphere field campaigns, Atmosphere, 10, doi:https://doi.org/10.3390/atmos10020066, 2019.

https://doi.org/10.5194/gmd-2021-88
Preprint. Discussion started: 25 May 2021


Prichard, S.J., Ottmar, R.D., and Anderson, G.K.: Consume 3.0 user's guide, http://www.fs.fed.us/pnw/fera/research/smoke/consume/consume30_users_guide.pdf, last access 19 October 2018, 2007.

Raj, P.K.: Large hydrocarbon fuel pool fires: Physical characteristics and thermal emission variations with height, J. Hazard. Mater., 140, 280-292, doi:https://doi.org/10.1016/j.jhazmat.2006.08.057, 2007a.

Raj, P.K.: LNG fires: A review of experimental results, models and hazard prediction challenges, J. Hazard. Mater., 140, 444-464, doi:https://doi.org/10.1016/j.jhazmat.2006.10.029, 2007b.

Ramsdale, S.A., Martin, D., Nikmo, J., Kukkonen, J., Liedtke, J., and Schatzmann, M.: Dispersion from strongly buoyant sources – overall executive summary, AEA Technology Report AEAT/1408, Warrington, 16 pp., 1997.

Randerson, J.T., Chen, Y., van der Werf, G.R., Rogers, B.M., and Morton, D.C.: Global burned area and biomass burning emissions from small fires, J. Geophys. Res., 117, G04012, doi:https://doi.org/10.1029/2012JG002128, 2012.

RDA: Research Data Archive, U.S. Department of Agriculture, https://www.fs.usda.gov/rds/archive/, last access 31 May 2018.

Rein, G.: Smoldering combustion, in: SFPE Handbook of Fire Protection Engineering, edited by Hurley, M.J., Fifth edition, ISBN 978-1-4939-2564-3, Springer Science+Business Media LLC New York, 581-603, doi:https://doi.org/10.1007/978-1-4939-2565-0_19, 2016.

Reinhardt, E.D., Keane, R.E., and Brown, J.K.: First Order Fire Effects Model: FOFEM 4.0, User's Guide, General Technical Report INT-GTR-344, Ogden, UT: U.S. Department of Agriculture, Forest Service, Intermountain Research Station, 65 pp., 1997.

Rew, P.J., and Hulbert, W.G.: Development of pool fire thermal radiation model, HSE Contract Research Report No. 96/1996, 62 p. + app, 1996.


Rew, P.J., Hulbert, W.G., and Deaves, D.M.: Modelling of thermal radiation from external hydrocarbon pool fires. Process Saf. Environ., 75, 81-89, doi:https://doi.org/10.1205/095758297528841, 1997.

Ricou, F.P., and Spalding, D.B.: Measurements of entrainment by axisymmetrical turbulent jets, J. Fluid Mech., 11, 21-32, doi:https://doi.org/10.1017/S0022112061000834, 1961.

Ross, J.L., Ferek, R.J., and Hobbs, P.V.: Particle and gas emissions from an in situ burn of crude oil on the ocean, J. Air Waste Manage., 46, 251-259, doi:https://doi.org/10.1080/10473289.1996.10467459, 1996.

Saarnio, K., Aurela, M., Timonen, H., Saarikoski, S., Teinilä, K., Mäkelä, T., Sofiev, M., Koskinen, J., Aalto, P.P., Kulmala, M., Kukkonen, J., and Hillamo, R.: Chemical composition of fine particles in fresh smoke plumes from boreal wild-land fires in Europe, Sci. Total Environ., 408, 2527-2542, https://doi.org/10.1016/j.scitotenv.2010.03.010, 2010.

Seiler, W., and Crutzen, P.J.: Estimates of gross and net fluxes of carbon between the biosphere and atmosphere from biomass burning. Climatic Change 2, 207-247, doi:https://doi.org/10.1007/BF00137988, 1980.

Seto, D., and Clements, C.B.: RxCADRE 2012: CSU-MAPS background wind, temperature, RH, and pressure time series data, Fort Collins, CO, Forest Service Research Data Archive, doi:https://doi.org/10.2737/RDS-2015-0027, 2015a.

Seto, D., and Clements, C.B.: RxCADRE 2012: CSU-MAPS wind LiDAR velocity and microwave temperature/relative humidity profiler data, Fort Collins, CO, Forest Service Research Data Archive, doi:https://doi.org/10.2737/RDS-2015-0026, 2015b.

Sofiev, M., Ermakova, T., and Vankevich, R.: Evaluation of the smoke-injection height from wild-land fires using remote-sensing data, Atmos. Chem. Phys., 12, 1995-2006, doi:https://doi.org/10.5194/acp-12-1995-2012, 2012.

https://doi.org/10.5194/gmd-2021-88
Preprint. Discussion started: 25 May 2021


Sofiev, M., Vankevich, M., Lotjonen, M., Prank, M., Petukhov, V., Ermakova, T., Koskinen, J., and Kukkonen, J.: An operational system for the assimilation of the satellite information on wild-land fires for the needs of air quality modelling and forecasting, Atmos. Chem. Phys., 9, 6833-6847, https://doi.org/10.5194/acp-9-6833-2009, 2009.

Soja, A.J., Cofer, W.R., Shugart, H.H., Sukhinin, A.I., Stackhouse Jr., P.W., McRae, D.J., and Conard, S.G.: Estimating fire emissions and disparities in boreal Siberia (1998-2002). J. Geophys. Res., 109, D14S06, doi:https://doi.org/10.1029/2004JD004570, 2004.

Strand, T., Gullett, B., Urbanski, S., O'Neill, S., Potter, B., Aurell, J., Holder, A., Larkin, N., Moore, M., and Rorig, M.: Grassland and forest understorey biomass emissions from prescribed fires in the southeastern United States - RxCADRE 2012, Int. J. Wildland Fire, 25, 102-113, doi:https://doi.org/10.1071/WF14166, 2016.

Tamanini, F.: Defining the effects of ambient conditions in large-scale fire tests, Exp. Therm. Fluid Sci., 34, 4040-411, doi:https://doi.org/10.1016/j.expthermflusci.2009.10.032, 2010.

Tang, T.: A physics-based approach to modeling wildland fire spread through porous fuel beds, Theses and Dissertations--Mechanical Engineering, 84, 236 pp., doi:https://doi.org/10.13023/ETD.2017.027, 2017.

Tewarson, A.: Heat release rate in fires. Fire Mater., 4, 85-191, doi:https://doi.org/10.1002/fam.810040405, 1980.

Tomppo, E., and Halme, M.: Using coarse scale forest variables as ancillary information and weighting of variables in k-NN estimation: a genetic algorithm approach, Remote Sens. Environ., 92, 1-20, doi:https://doi.org/10.1016/j.rse.2004.04.003, 2004.

https://doi.org/10.5194/gmd-2021-88
Preprint. Discussion started: 25 May 2021




Trentmann, J., Andreae, M. O., Graf, H.-F., Hobbs, P.V., Ottmar, R.D., and Trautmann, T.: Simulation of a biomass-burning plume: Comparison of model results with observations, J. Geophys. Res., 107, AAC5.1–AAC5.15, doi:https://doi.org/10.1029/2001JD000410, 2002.

Trentmann, J., Luderer, G., Winterrath, T., Fromm, M.D., Servranckx, R., Textor, C., Herzog, M., Graf, H.-F., and Andreae, M.O.: Modeling of biomass smoke injection into the lower stratosphere by a large forest fire (Part I): reference simulation, Atmos. Chem. Phys., 6, 5247-5260, doi:https://doi.org/10.5194/acp-6-5247-2006, 2006.

Urbanski, S.: Wildland fire emissions, carbon, and climate: Emission factors, Forest Ecol. Manag., 317, 51-60, doi:https://doi.org/10.1016/j.foreco.2013.05.045, 2014a.

Urbanski, S.P.: RxCADRE 2012: Airborne measurements of smoke emission and dispersion from prescribed fires, Fort Collins, CO, Forest Service Research Data Archive, doi:https://doi.org/10.2737/RDS-2014-0015, 2014b.

van der Werf, G.R., Randerson, J.T., Collatz, G.J., and Giglio, L.: Carbon emissions from fires in tropical and subtropical ecosystems, Glob. Change Biol., 9, 547-562, doi:https://doi.org/10.1046/j.1365-2486.2003.00604.x, 2003.

van der Werf, G.R., Randerson, J.T., Giglio, L., Collatz, G.J., Mu, M., Kasibhatla, P.S., Morton, D.C., DeFries, R.S., Jin, Y., and van Leeuwen, T.T.: Global fire emissions and the contribution of deforestation, savanna, forest, agricultural, and peat fires (1997-2009), Atmos. Chem. Phys., 10, 11707-11735, doi:https://doi.org/10.5194/acp-10-11707-2010, 2010.

Venäläinen, A., Laapas, M., Pirinen, P., Horttanainen, M., Hyvönen, R., Lehtonen, I., Junila, P., Hou, M., and Peltola, H.M.: Estimation of the high-spatial-resolution variability in extreme wind speeds for forestry applications, Earth Syst. Dynam., 8, 529-545, doi:https://doi.org/10.5194/esd-8-529-2017, 2017.

Virkkula, A., Levula, J., Pohja, T., Aalto, P.P., Keronen, P., Schobesberger, S., Clements, C.B., Pirjola, L., Kieloaho, A.-J., Kulmala, L., Aaltonen, H., Patokoski, J., Pumpanen, J., Rinne, J., Ruuskanen, T.,

https://doi.org/10.5194/gmd-2021-88
Preprint. Discussion started: 25 May 2021




Pihlatie, M., Manninen, H.E., Aaltonen, V., Junninen, H., Petäjä, T., Backman, J., Dal Maso, M., Nieminen, T., Olsson, T., Grönholm, T., Aalto, J., Virtanen, T. H., Kajos, M., Kerminen, V.-M., Schultz, D. M., Kukkonen, J., Sofiev, M., De Leeuw, G., Bäck, J., Hari, P., and Kulmala, M.: Prescribed burning of logging slash in the boreal forest of Finland: emis sions and effects on meteorological quantities and soil properties, Atmos. Chem. Phys., 14, 4473-4502, doi:https://doi.org/10.5194/acp-14-4473-2014, 2014a.

Virkkula, A., Pohja, T., Aalto, P.P., Keronen, P., Schobesberger, S., Clements, C.B., Petäjä, T., Nikmo, J., and Kulmala, M.: Airborne measurements of aerosols and carbon dioxide during a prescribed fire experiment at a boreal forest site, Boreal Environ. Res., 19, 153-181, 2014b.

Wiedinmyer, C., Quayle, B., Geron, C., Belote, A., McKenzie, D., Zhange, X., O'Neill, S., and Wynne, K.K.: Estimating emissions from fires in North America for air quality modeling, Atmos. Environ., 40, 3419-3432, doi:https://doi.org/10.1016/j.atmosenv.2006.02.010, 2006.

Zabetakis, M.G., and Burgess, D.S.: Research on the hazards associated with the production and handling of liquid hydrogen. Technical report BM-RI-5707, Bureau of Mines, Washington, D.C., USA, 50 p., doi:https://doi.org/10.2172/5206437, 1961.

Zukoski, E.E., Cetegen, B.M., and Kubota, T.: Visible structure of buoyant diffusion flames, Symposium (International) on Combustion, 20, 361-366, doi:https://doi.org/10.1016/S0082-0784(85)80522-1, 1985.